ENDOPLASMIC RETICULUM STRESS-INDUCED APOPTOSIS RESISTANCE MECHANISMS IN IDIOPATHIC PULMONARY FIBROSIS-DERIVED FIBROBLASTS

by

Durwood Moore

A Thesis
Submitted to the
Graduate Faculty
of
George Mason University
in Partial Fulfillment of
The Requirements for the Degree
of
Master of Science
Biology

Committee:

_____ Dr. Geraldine Grant, Thesis Chair

_____ Dr. Luis Rodriguez, Committee Member

_____ Dr. Charles Madden, Committee Member

_____ Dr. Iosif Vaisman, Director,
School of Systems Biology

_____ Dr. Gerald L. R. Weatherspoon, Associate Dean for Undergraduate and Graduate Affairs, College of Science

_____ Dr. Fernando R. Miralles-Wilhelm, Dean, College of Science

Date: _____ Spring Semester 2024
George Mason University
Fairfax, VA

Endoplasmic Reticulum Stress-Induced Apoptosis Resistance Mechanisms in Idiopathic Pulmonary Fibrosis-Derived Fibroblasts

A Thesis submitted in partial fulfillment of the requirements for the degree of Master of Science at George Mason University

by

Durwood Moore
Bachelor of Science
George Mason University, 2019

Director: Geraldine Grant, Department Chair
Department of Biology

Spring Semester 2024
George Mason University
Fairfax, VA

DEDICATION

This work is dedicated to the patients and families whose lives have been forever changed by idiopathic pulmonary fibrosis.

ACKNOWLEDGMENTS

I would like to thank my committee chair, Dr. Geraldine Grant, for her support and guidance over the last several years. I also wish to thank committee member, Dr. Luis Rodriguez, for his mentorship, technical assistance, and guidance. I would also like to thank committee member, Dr. Charles Madden, for his valuable input during the defense and writing process. Thank you to George Mason University for making me feel at home for the last several years. I would be remiss if I didn't thank my family, for their unquestioning support, and my parents, Nadean Moore and Durwood Moore Sr. for providing me with the opportunity to succeed and always encouraging me to ask 'why?'.

TABLE OF CONTENTS

LIST OF FIGURES

LIST OF ABBREVIATIONS AND SYMBOLS

AT2 ..... Alveolar type 2 cell
ATF-6 ..... Activating transcription factor 6
BI-1 ..... BAX Inhibitor 1
BiP ..... Binding immunoglobulin protein
β-GAL ..... Beta-galactosidase
CASP3 ..... Caspase 3
CHOP ..... C/EBP homologous protein
DNA ..... Deoxyribonucleic acid
ECM ..... Extracellular matrix
ER ..... Endoplasmic reticulum
ERAD ..... ER-associated degradation
ERO1A ..... ER oxidoreductase 1 alpha
ERSE ..... ER stress response element
HO1 ..... Heme oxygenase 1
IHC ..... Immunohistochemistry
IL-1β ..... Interleukin 1 beta
IL-6 ..... Interleukin 6
IL-8 ..... Interleukin 8
IPF ..... Idiopathic pulmonary fibrosis
IPF-F ..... IPF fibroblasts
IRE1α ..... Inositol-requiring enzyme 1 alpha
mRNA ..... Messenger RNA
NHLF ..... Normal human lung fibroblasts
PERK ..... Protein kinase R-like ER kinase
RIDD ..... Regulated IRE1α-dependent decay
RNA ..... Ribonucleic acid
ROS ..... Reactive oxygen species
SASP ..... Senescence-associated secretory phenotype
siRNA ..... Small interfering RNA
SNP ..... Single nucleotide polymorphism
sXBP-1 ..... spliced XBP-1
TGF-β ..... Tumor growth factor beta
Tm ..... Tunicamycin
TNF-α ..... Tumor necrosis factor-alpha
UPR ..... Unfolded protein response
uXBP-1 ..... unspliced XBP-1
XBP-1 ..... X-box binding protein 1

ABSTRACT

ENDOPLASMIC RETICULUM STRESS-INDUCED APOPTOSIS RESISTANCE MECHANISMS IN IDIOPATHIC PULMONARY FIBROSIS-DERIVED FIBROBLASTS

Durwood Moore, M.S.

George Mason University, 2025

Thesis Director: Geraldine Grant

Idiopathic pulmonary fibrosis (IPF) is a devastating fatal interstitial lung disease that is the result of an accumulation of highly secretory senescent fibroblasts. Our group has previously demonstrated that IPF fibroblasts (IPF-F) are resistant to the apoptotic pressures initiated by the unfolded protein response (UPR) during times of ER stress. IPF-F show an upregulation of BAX Inhibitor-1 (BI-1), which has been shown to negatively regulate the dimerization of IRE1α and inhibit BAX-mediated apoptosis. We hypothesize that IPF-F can evade ER stress-induced apoptosis through an upregulation of BI-1, but it is uncertain whether this is primarily through an IRE1α or BAX-driven pathway.

IPF-F and normal human lung fibroblasts (NHLF) were transfected with siRNAs targeting BI-1, IRE1α, and BAX. ER stress was generated through a 0.1 μg/mL tunicamycin challenge. Activation of ER stress-driven apoptosis was assayed through a

western blot of apoptosis signaling molecules CHOP and Caspase 3. Cell survival was measured through a CCK-8 cytotoxicity assay.

We demonstrate that both the IRE1α and BAX pathways are important to the cell's ability to undergo ER stress-driven apoptosis. Silencing each pathway individually did not rescue the cell from tunicamycin-induced apoptosis. This suggests that BI-1 is a multifaceted inhibitor of ER stress-mediated apoptosis. Further characterization of UPR and BAX-driven apoptosis via western blot will be required to better understand the mechanisms by which BI-1 prevents apoptosis.

INTRODUCTION

Background

Idiopathic pulmonary fibrosis (IPF) is a fatal, age-related, interstitial lung disease of unknown origin with no known cure [1,2]. IPF is thought to be the result of a dysfunctional wound repair process, catalyzed by an accumulation of apoptosis-resistant senescent fibroblasts, which results in progressive scarring within the interstitium of the lung [1,2]. IPF typically begins in the lower periphery of the lung and slowly progresses until the architecture of the entire lung is disrupted [1–3]. The prognosis for patients with IPF is inevitably dire due to a lack of effective treatment options, with the time between the onset of symptoms to diagnosis to death being 3-5 years on average [4]. In the United States, the prevalence of IPF is estimated to be 50 per 100,000, but this number varies greatly depending on age [1,4,5]. In patients over the age of 65 years, the prevalence increases to 400 per 100,000 [1,4,5]. With the global population aging at a rapid rate and the most recent IPF therapeutic being approved in 2015, there is an urgent need for the discovery and approval of new therapies.

While the precise cause for IPF development is largely unknown, there is a favored mechanism of pathogenesis in the field at large that involves three main steps: predisposition, initiation, and progression (Figure 1). In this model, an aging, genetically susceptible lung is exposed to repeated subclinical injuries, resulting in profibrotic

epigenetic changes in the alveolar epithelium. Damage to the epithelium triggers the release of pro-inflammatory cytokines, like TGF-β, TNF-α, IL-1β, IL-6, and IL-8. These important signaling molecules promote lung fibroblast recruitment, proliferation, and differentiation into myofibroblasts, which are responsible for depositing excessive collagen into the interstitial space. Dysfunctional crosstalk between these myofibroblasts, alveolar epithelium, and recruited immune cells results in the propagation and progression of the pro-inflammatory signal, leading to continued myofibroblast activation, extracellular matrix (ECM) deposition, and lung scarring [1,4,6].

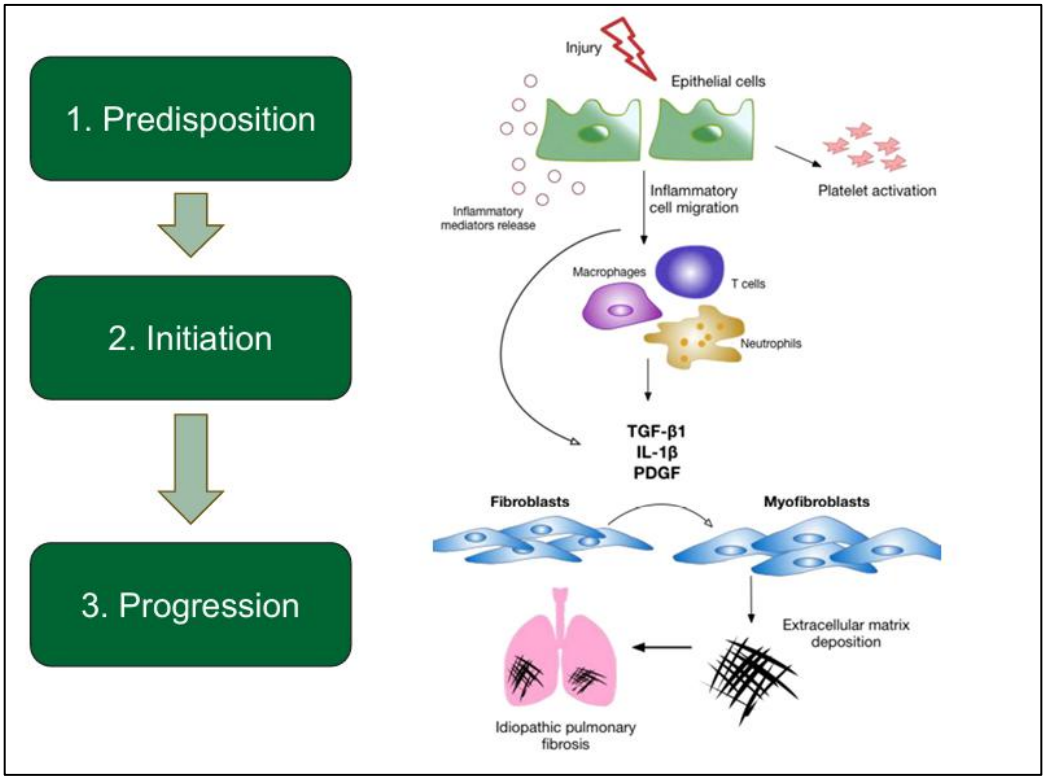

Figure 1: Idiopathic pulmonary fibrosis pathogenesis model.
Adapted from Wolters *et al.* to demonstrate the proposed model of IPF pathogenesis. Subclinical injuries to a genetically predisposed, aging epithelium attract immune cells to the area of damage. Proinflammatory cytokines recruit fibroblasts to initiate a wound repair response. These fibroblasts differentiate into myofibroblasts, which secrete extracellular matrix into the interstitial space. Dysfunctional crosstalk between the epithelium, immune cells, and fibroblasts results in excessive amounts of inflammation and collagen production in the interstitium.

Risk factors

Though the cause of IPF is unknown, several factors have been identified that increase the risk of developing the disease. A study conducted by Fell et al. demonstrated that age was one of the largest positive predictor values for patients with IPF [7]. Genetics also plays a key role in the development of IPF. Variants of the *TERT* and *TERC* genes, along with several other telomere maintenance genes, have been found in one-fourth of familial IPF patients. It has been shown that these mutations contribute to significantly shorter telomeres in alveolar epithelial type 2 (AT2) cells in the lungs of both familial and sporadic IPF patients [1,4,6]. Mutations in surfactant protein C, which is exclusively expressed by AT2 cells, have been linked to interstitial lung disease as well. In 2011, a genome-wide study identified the single-nucleotide polymorphism (SNP) rs35705950, located 3 kb upstream of the gene *MUC5B,* which encodes a glycoprotein essential for normal mucus clearance. This SNP is present in 34% of patients with IPF and is associated with a 37.4 times increase in *MUC5B* expression [8]. It is thought that these mutations prevent the proper folding of the peptide, which can lead to a loss of proteostasis, an increase in ER stress, and may even promote epithelial-mesenchymal transition (EMT) [4,8].

Occupational exposures, such as agricultural, farming, wood dust, metal dust, and silica are shown to increase the risk of developing IPF, but cigarette smoke has been identified as the most common source of irritation to the lung epithelium [1,4,6].

Aging and Senescence

As we grow older, our bodies experience a gradual decline in biological functions, making us more susceptible to various diseases such as pulmonary fibrosis, cancers, and neurodegenerative diseases [9–11]. This is why aging is considered the biggest risk factor for many human illnesses. With significant advancements in medicine and public health in the last century, the global population is aging at an unprecedented rate. In fact, as of 2018, the number of adults over 64 years old has surpassed that of children under 5 years old, and by 2050, it is estimated that nearly 20% of the world's population will be over the age of 65 [12].

According to Lopez-Otin et al., twelve cellular and molecular hallmarks of aging are widely recognized (Figure 2) [9]. Although interconnected, the hallmarks of aging can be divided into three categories. Cellular changes that initiate a damage response are known as primary hallmarks, and these include telomere attrition, epigenetic alterations, and loss of proteostasis. Responses to these primary hallmarks, like mitochondrial dysfunction and cellular senescence, are known as antagonistic hallmarks. When the damage caused by the primary and antagonistic hallmarks cannot be regulated through normal homeostatic mechanisms, integrative hallmarks begin to appear. These include stem cell exhaustion, altered intercellular communication, and chronic inflammation [9].

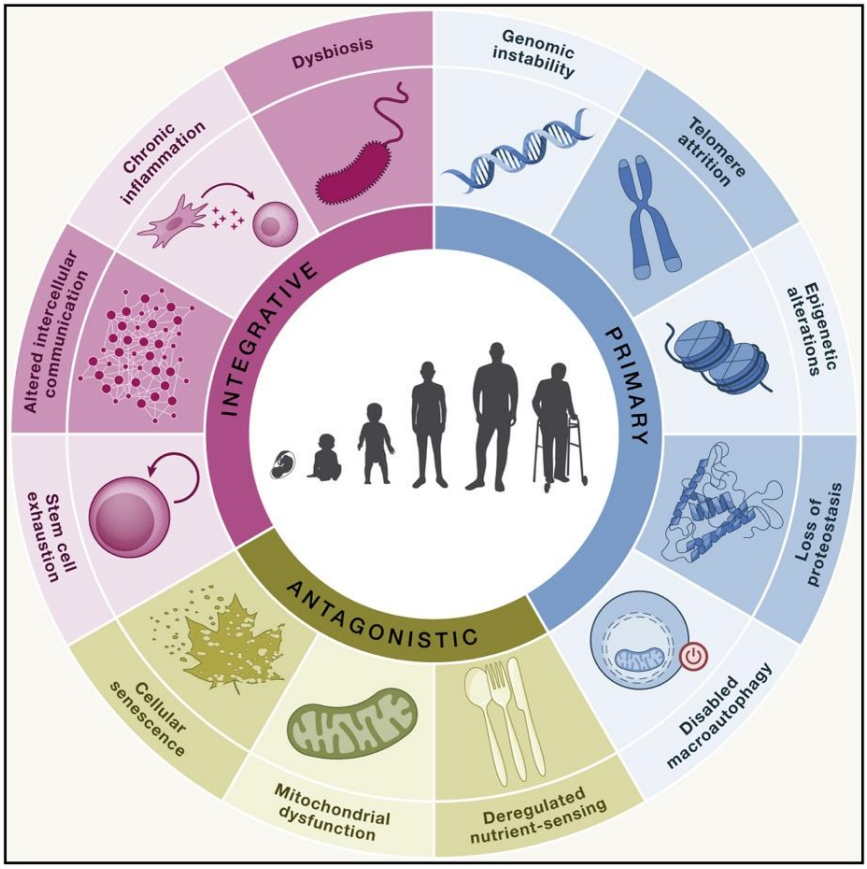

Figure 2: The biological hallmarks of aging.
Illustration[9] shows the 12 pillars of biological aging. Primary hallmarks directly cause damage at the cellular level, which accumulates to trigger antagonistic hallmarks in response to the damage. When antagonistic hallmarks are unable to be mitigated by normal homeostatic mechanisms, integrative hallmarks emerge, leading to tissue and organ dysfunction.

Studies have shown that epithelial and mesenchymal cells in the IPF lung exhibit higher rates of cellular senescence than in a healthy lung [13,14]. Cellular senescence is a state of permanent cell cycle arrest that can be initiated by various endogenous factors, like DNA damage and reactive oxygen species (ROS), and some exogenous factors[13–17]. Its primary purpose is to protect against the proliferation of aged cells that have increased potential to form tumors. Senescent cells are resistant to apoptosis-inducing stimuli, and key regulatory proteins like p53, p21, p16, and p19 are responsible for permanently

blocking the cell cycle [15–17]. Cellular senescence plays a critical role during embryonic development, tumor suppression, and tissue repair. However, an unregulated accumulation of senescent cells is observed in many age-related diseases, particularly IPF [13,14]. Senescent cells also exhibit the senescence-associated secretory phenotype (SASP), which involves the secretion of growth factors, cytokines, extracellular matrix, and extracellular matrix remodeling factors. Through these secreted factors, senescent cells can recruit immune cells, activate nearby fibroblasts, and induce neighboring cells to enter senescence [15–17].

Endoplasmic Reticulum Stress and the Unfolded Protein Response

The synthesis and folding of proteins that will eventually be secreted by the cell takes place in the endoplasmic reticulum (ER)[18–20]. The ER's lumen is highly sensitive to perturbations in chaperone availability, nutrient deprivation, hypoxia, and oxidative stress [18,20]. In a hypoxic environment such as the IPF lung, highly secretory cells, like senescent cells with the SASP, can be vulnerable to the accumulation of ROS-damaged proteins. These oxidatively damaged proteins aggregate within the ER disrupting cellular proteostasis known as ER stress [18–20]. Genetic alterations that prevent proper protein folding, like the *SFTPC* mutation common in IPF, can also induce ER stress [21]. Prolonged ER stress is lethal to cells, a process known as ER stress-induced apoptosis, which is typically mediated through the proapoptotic protein BAX. To combat the negative effects of ER stress, cells have adaptive response mechanisms that are collectively known as the unfolded protein response (UPR) [18–20].

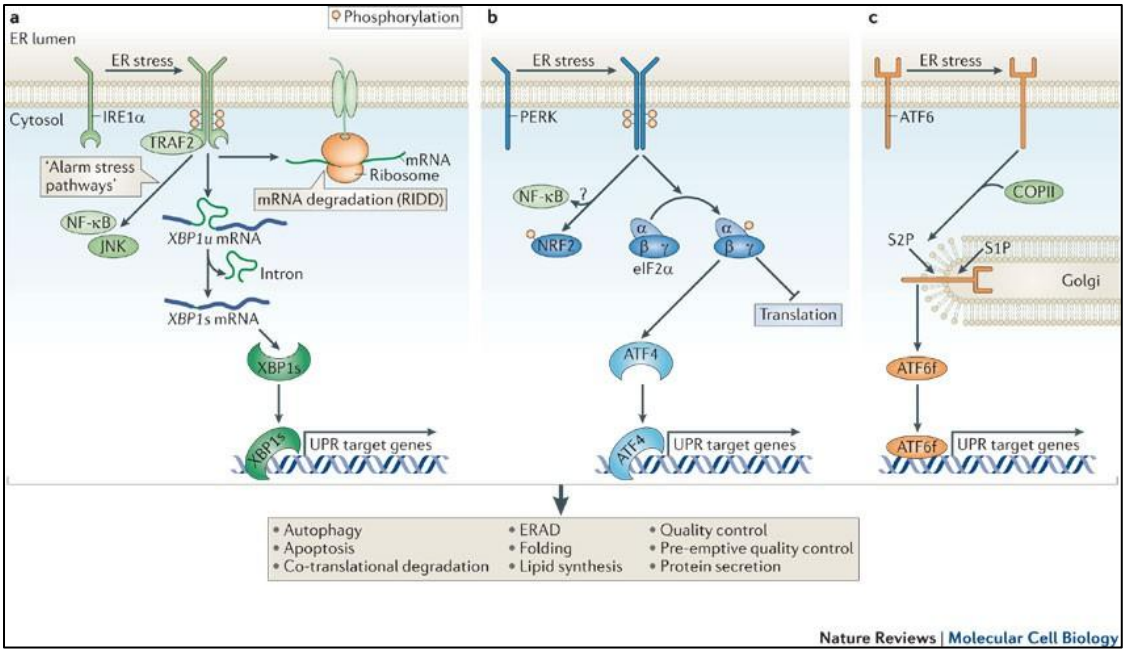

Figure 3: The unfolded protein response (UPR)
Illustration[22] shows the three signaling pathways comprising the unfolded protein response: inositol-requiring enzyme 1 alpha (IRE1α), pancreatic ER kinase (PERK), and activating transcription factor-6 (ATF6). An accumulation of unfolded protein activates these three pathways, leading to mRNA degradation, translation inhibition, and increased chaperone expression, among other responses.

The UPR has three canonical pathways used to overcome the accumulation of unfolded proteins in the ER lumen (Figure 3): pancreatic ER kinase (PERK), activating transcription factor-6 (ATF6), and inositol-requiring enzyme 1 (IRE1). These three receptors are maintained in an inactive state in unstressed cells through an association with the ER chaperone, binding immunoglobulin protein (BiP) [18–20,22]. Under ER stress conditions, BiP preferentially binds to the accumulating unfolded protein by dissociating and activating the three UPR receptors. UPR activation is recognized through three different types of responses: a decrease in the rate of protein synthesis, an increase in the rate of protein folding, and an increase in the degradation of misfolded proteins [18–20,22].

PERK

The dissociation of BiP allows PERK monomers to dimerize and autophosphorylate. This active form of PERK phosphorylates eukaryotic initiation factor 2-alpha (eIF2α), which prevents general protein translation, reducing the rate of protein synthesis. By decreasing the number of nascent proteins entering the ER, the stress is alleviated, and cell survival is promoted, hence, eIF2α activation promotes cell survival. PERK activation does not prevent the translation of all proteins; some genes carry regulatory sequences that can circumvent the eIF2α translational block. *ATF4* is one of these genes and encodes a cAMP response element binding transcription factor (C/EBP). Activated, translated ATF4 translocates to the nucleus and induces transcription of genes related to amino-acid metabolism, redox reactions, stress response, and protein secretion [19]. ATF4 also induces the transcription of the transcription factor C/EBP homologous protein (CHOP), a well-known initiator of BAX-induced apoptosis signaling [19,22].

ATF6

Upon the dissociation of BiP, ATF6 translocates to the Golgi apparatus, where it is cleaved into an active form by proteases. The now-active form of ATF6 once again translocates to the nucleus and induces the transcription of the ER stress response element (ERSE). ER chaperone proteins BiP, GRP94, and protein disulfide isomerase, along with additional transcription factors CHOP and X box-binding protein 1 (XBP-1) are controlled by the ERSE [19].

IRE1

IRE1α is a transmembrane dual-activity enzyme localized in the ER. Like PERK, IRE1α has a cytosolic serine/threonine kinase domain, but it also has a unique endoribonuclease domain. When IRE1α oligomerizes in the absence of BiP, it autophosphorylates and begins to splice a 26-nucleotide intron from the XBP-1 mRNA, which is upregulated by ATF6. This results in an active transcription factor known as spliced XBP-1 (sXBP-1), which translocates to the nucleus and induces the upregulation of ER-associated degradation and lipid biosynthesis genes [18,19,22]. The unspliced form of XBP-1 (uXBP-1) is unable to act as a transcription factor but instead acts as a negative feedback regulator by targeting ATF6 for proteasomal degradation [23].

BAX Inhibitor-1: Potential UPR Regulatory Protein

The most widely recognized regulator of the UPR is BiP, but it has been observed that BiP is not the sole regulator of the activity of IRE1α [24]. BAX Inhibitor-1 (BI-1) has been shown to be a negative regulator of the ER stress sensor IRE1α and a suppressor of BAX-mediated apoptotic signaling [25,26]. BI-1 is a six-transmembrane domain-containing protein located primarily in the ER. BI-1 was named for its physical interaction with BCL-2-related proteins that regulate BAX-mediated apoptosis. The regulation of BAX-mediated apoptosis by BI-1 has been shown not to involve direct protein-protein interactions [26,27]. IRE1α activity has also been shown to be repressed by BI-1 expression in drosophila and mouse models of ER stress through the formation of a complex with IRE1α monomers. This complex formation would prevent effective dimerization and inhibit IREα endoribonuclease activity [25].

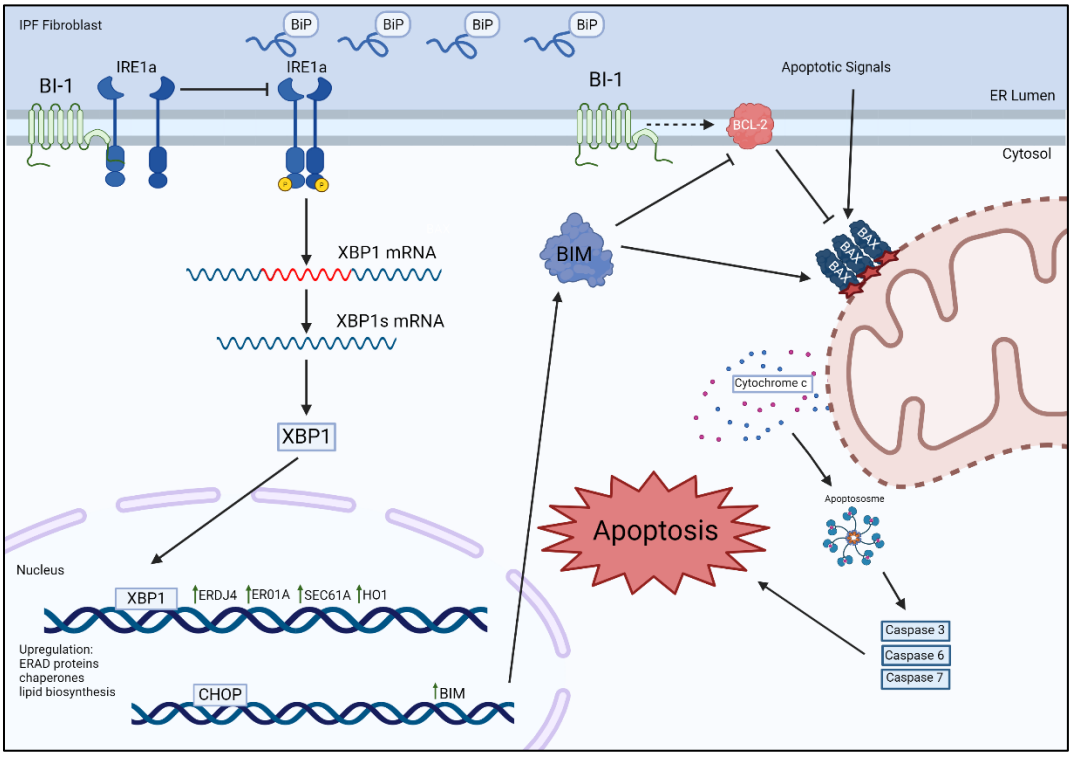

Figure 4: Proposed mechanism of action for BAX Inhibitor-1 (BI-1)
BAX Inhibitor-1 is thought to be a negative regulator of IRE1α by interacting with the cytosolic domain, preventing effective dimerization during conditions of ER stress. This would prevent the splicing of XBP-1, upregulation of some UPR target genes, and downstream pro-apoptosis signaling. BI-1 is also known to inhibit BAX-mediated apoptosis by interacting with the anti-apoptotic protein BCL-2, though the exact mechanism is not entirely known.

METHODS

Materials

All chemicals and supplies were purchased from Fisher Scientific (Pittsburgh, PA) unless specified. Antibodies were purchased from Abcam (Cambridge, MA), and primers from Invitrogen (Carlsbad, CA). Human lung fibroblasts MRC-5 (CCL-171) and lung epithelial cells A549 (CCL-185) were obtained from the American Type Culture Collection (ATCC, Manassas, VA).

Donor lung procurement

Lung samples (IPF and normal) were obtained from Inova Fairfax Medical Campus and the Washington Regional Transplant Community (WRTC) respectively, under approved investigative protocols (Inova Health System and George Mason University Institutional Review Boards).

Primary fibroblast isolation and culture

IPF-F and NHLF were isolated from lung tissue by enzymatic dissociation and differential binding. The lungs were oriented from apex to base and all samples used in this study were taken from the peripheral lower lobe of the lung. Briefly, samples were dissected into 1-2 mm^2 pieces and subjected to enzymatic digestion in 0.4% collagenase P (Roche, Indianapolis, IN) complete media (Dulbecco Minimal Essential Media (DMEM) containing 10% fetal bovine serum (FBS), penicillin (100 I.U/mL), streptomycin (100 MCH/mL) amphotericin B (0.25 M.C.G./mL P/S/A) and 0.1% DNase1), at 37°C and 5% CO_2 for 2 hours. The resulting material was passed through

sterile cell filters (40, 100 μ nylon mesh) to remove undigested tissue and the remaining cells were pelleted by centrifugation at 1000 g for 5 minutes. The pelleted cells were then suspended in complete media and seeded onto tissue culture-treated plastic at 37°C and 5% CO_2 for 45 minutes. The attached fibroblast population was vigorously washed with PBS to remove any attached cells.

β-Galactosidase staining

β-Galactosidase staining was performed using the β-Galactosidase staining kit from Abcam. Briefly, cells were washed with PBS and fixed in paraformaldehyde for 10 minutes at room temperature. After fixation, cells were washed again and incubated with the staining solution mixture which contains X-gal at 37°C and 0% CO_2 for 1 hour. Following staining, cells were washed with PBS and observed under an EVOS FL Auto microscope.

siRNA transfection

Cells were seeded onto 6-well and 96-well tissue culture-treated plastic dishes and grown to 70% confluency. Transfection complexes were prepared according to ThermoFisher Lipofectamine RNAiMAX transfection kit protocols. siRNA targets were BAX inhibitor 1, IRE1α, and BAX. Transfection complexes were added dropwise to cell dishes and incubated for 24 hours at 37°C and 5% CO_2.

qPCR

HO1, ERO1A, SEC61A, ERdj4, BiP, p21, p16, and Cyclin D, were assessed by quantitative real-time PCR (qPCR). Total RNA (1μg) was reverse transcribed to cDNA using the iScript cDNA synthesis kit (BioRad). qPCR was carried out using Quantifast

SYBR green PCR kit (Qiagen). All gene expressions were normalized to 18S gene expression using the Comparative Ct 2-(delta)(delta)Ct method (Pfaffl, 2001)

Western blotting

20µg of total cellular protein was subjected to gel electrophoresis using a 4-12% Bis-Tris gradient gel (Invitrogen). Visible molecular weight markers were included (Pre-Stained Protein Ladder, Fisher). Proteins were transferred to the nitrocellulose membrane using the iBLOT® system (Invitrogen). All membranes were blocked with 5% non-fat dried milk in Tris-buffered saline (TBS) containing 0.1% Tween-20 (TBS-T) for 1 hour at room temperature. After blocking, the TBS-T was replaced with TBS-T 5% non-fat dried milk containing primary antibodies (Cell Signaling) at a concentration of 1µg/ml of each antibody overnight at 4°C. After overnight incubation each membrane was washed 5 times for 5 minutes (5x5mins) with TBS-T, followed by incubation with the appropriate horseradish peroxidase (HRP)-linked secondary antibodies in TBS-T 5% non-fat dried milk for 1 hour at room temperature. Afterward, each membrane was washed with TBS-T 5X5min then visualized by incubation with chemiluminescent Super Signal West Femto Max Sensitivity Substrate (Pierce). For normalization, blots were then stripped using Restore Western Blot Stripping Buffer (Thermo Scientific) according to the manufacturer's protocol. Each membrane was then re-probed with a primary antibody and secondary antibody as previously described. All immunoblots were imaged using ChemiDoc™ XRS System (Bio-Rad) and densitometry analysis was performed using ImageJ. Protein expression was normalized to beta-actin (ab 8227, Abcam), COXIV (ab

4844, Cell Signaling), GAPDH (ab 5174, Cell Signaling) or beta-tubulin (ab 2146, Cell Signaling) expression.

Cell viability

Cells were seeded onto 96 well tissue culture-treated plastic dishes at a density of 5000 cells/well. Plates were incubated for 24 hours before receiving treatments of 0.1 μg/mL tunicamycin, siRNA transfection reagents, or a combination of both 0.1 μg/mL tunicamycin and siRNA transfection reagents. Following incubation with treatments, culture media was replaced with Cell Counting Kit-8 solution (APExBIO, Houston, TX) diluted 1:10 in complete media. Plates were incubated for 2 hours at 37°C and 5% CO_2 before measuring absorbance at 450 nm

Total protein extraction

Total cellular protein was isolated using RIPA buffer (Pierce), with the addition of complete mini protease inhibitor cocktail tablets (Roche) and PhosSTOP™ phosphatase inhibitors cocktail tablets (Roche) per the manufacturer's instructions. Lysed cells were centrifuged at 13,000Xg for 20 minutes to remove cellular debris. The resulting supernatant was collected and stored at -80°C. Total protein concentration was determined by the Pierce BCA Protein Assay Kit.

Total RNA extraction

Total RNA was extracted using the RNeasy® Kit (Qiagen) from treated and untreated control cells. All RNA was quantified using a Nanodrop™ spectrophotometer (NanoDrop™ One, Thermo Scientific) and stored at -80°C.

Statistical analysis

Statistical analyses were carried out using Prism 3.03 software (GraphPad). Two-way ANOVA with Tukey's posthoc multiple comparisons were performed for all analyses unless otherwise stated in the figure caption. All data presented are representative of experiments performed at least in triplicate. A p-value less than 0.05 was considered significant. * indicates p-value less than 0.05, ** indicates p-value less than 0.01, *** indicates p-value less than 0.001 between groups.

PRELIMINARY STUDIES AND HYPOTHESIS

Rationale

Since the role of BAX Inhibitor-1 in IPF fibroblasts remains largely unknown, a series of preliminary studies was first used to develop hypotheses and optimize techniques on primary cell populations. The goal of these preliminary studies was to characterize the cell populations being cultured relative to the field at large, determine BI-1 expression within the IPF lung, investigate basal UPR activity within IPF-F and NHLF, and optimize siRNA transfection and ER stress challenge conditions.

IPF fibroblasts display increased markers of senescence

Prior to characterizing the effect of BI-1 on the IRE1α arm of the UPR, the basal phenotype of the IPF-F being cultured had to be confirmed. The fibrosis field at large has determined that IPF-F are more senescent and resistant to apoptosis than their normal counterparts [13,15,17]. To verify this, a β-galactosidase (β-gal) staining assay was performed on passage-matched IPF-F and NHLF. Normal fibroblasts displayed less than 1% positive β-gal signal, while IPF-F showed 90% positive staining (Figure 5A, B). Telomere length was also measured via PCR, revealing that IPF-F have significantly shorter telomeres than normal, by approximately 80 kb/genome (Figure 5C).

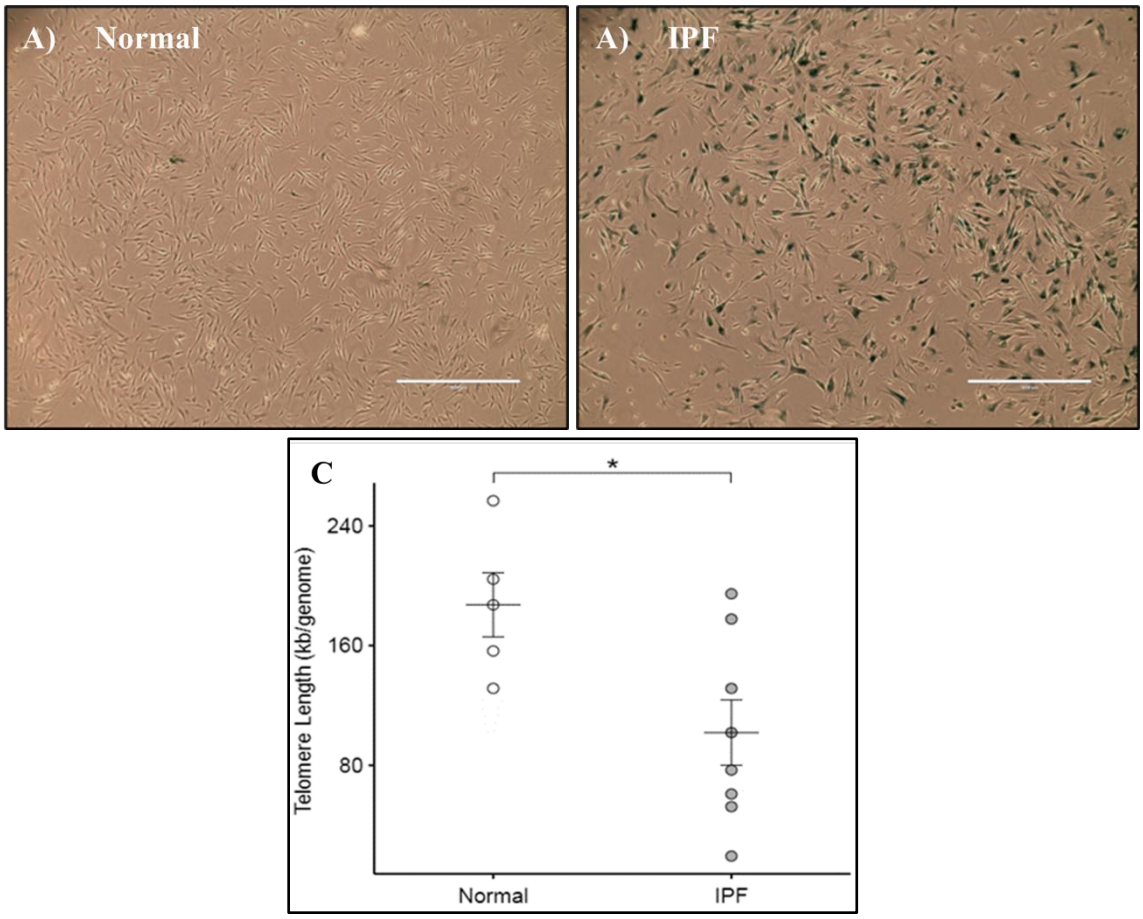

Figure 5: Beta-galactosidase staining and telomere attrition in NHLF and IPF-F
Senescence in NHLF and IPF-F was assessed by: **A-B)** β-gal staining. A representative picture of the comparison is shown for normal **(A)** and IPF **(B)** taken at 20X magnification with blue-green cells indicating a positive marker of senescence. **C)** Telomere lengths of age-matched and passage-matched primary fibroblasts were measured using qPCR.

IPF fibroblasts display cell cycle arrest and an anti-apoptotic phenotype

Since senescent cells are known to exit the cell cycle, gene expression of important cell cycle regulators p21 and Cyclin D were measured via qPCR. IPF-F have a 10-fold increase in the expression of p21 and an 8-fold decrease in the expression of Cyclin D compared to NHLF, pointing to cell cycle arrest. In addition, senescent cells are also known to be resistant to apoptosis. The negative regulator of apoptosis, Bcl-xL was also measured via qPCR, revealing increased expression in IPF-F (Figure 6A). Protein

expression analysis also showed an increase in Bcl-xL in IPF-F compared to NHLF (Figure 6B). Combined with β-gal staining and telomere length, these data verify that the IPF-F being cultured show an increased senescent and anti-apoptotic phenotype.

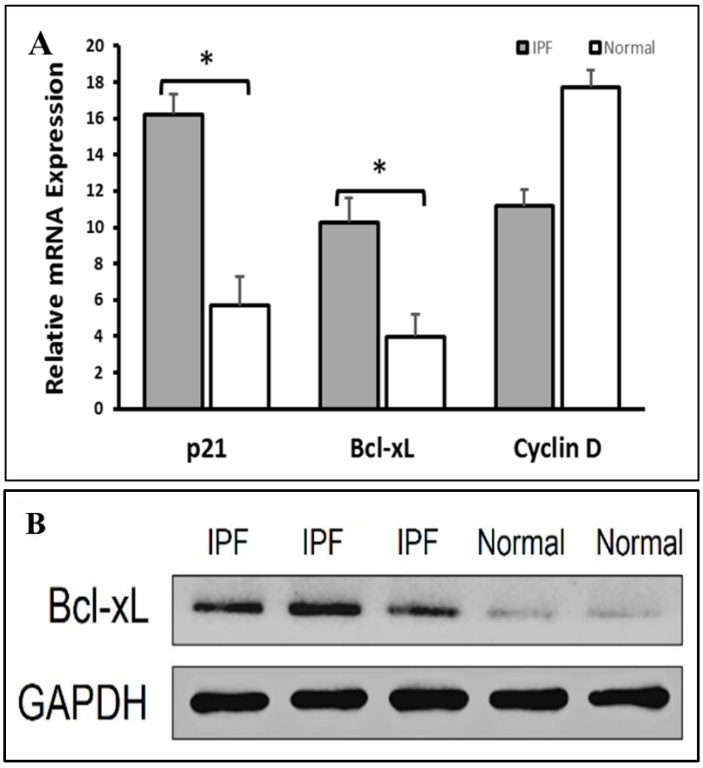

Figure 6: Gene expression of markers associated with senescence and BcL-xL pro-survival protein expression. A) qPCR of RNA isolated from normal (n=4) and IPF (n=4) fibroblasts was used to measure the relative expression of genes related to replication (Cyclin D), apoptosis resistance (BcL-xL), and senescence (p21) normalized to 18S expression.

BI-1 expression is increased in IPF-F

Since BI-1 has been shown by other groups to play a role in senescent cells[28], BI-1 may be playing a similar in IPF. To determine if BI-1 is expressed in the IPF lung, immunohistochemistry (IHC) targeting was performed, showing that IPF donor lung

tissue has increased expression of BI-1 compared to normal lung tissue. Gene expression analysis of IPF-F isolated from donor lung tissue showed a 7-fold increase in BI-1 expression relative to NHLF (Figure 7).

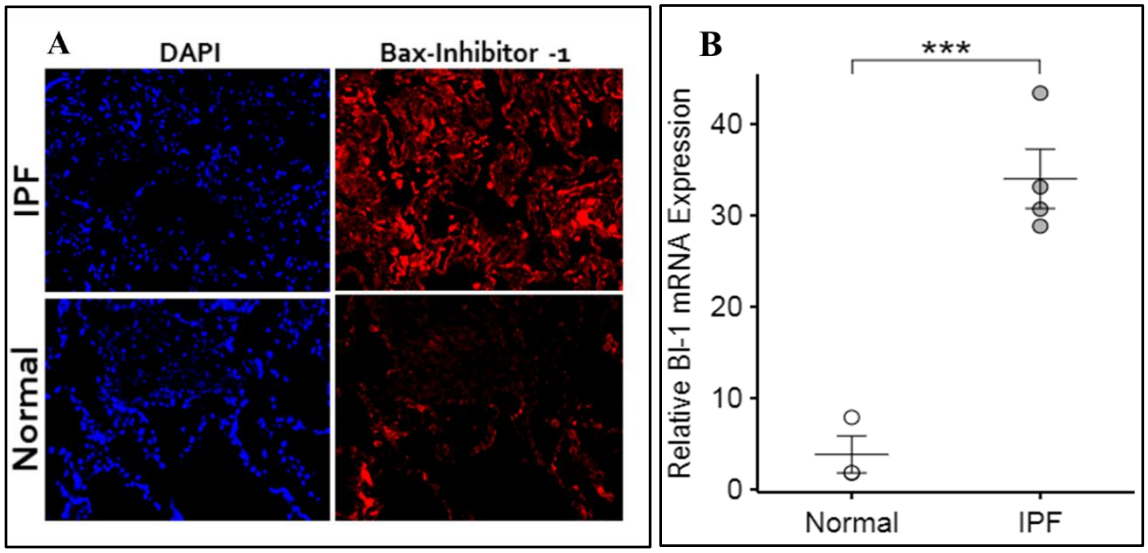

Figure 7: BAX-Inhibitor 1 expression in IPF and normal lung sections and fibroblasts.
A) Lung tissue sections from IPF and normal patients were probed for BAX Inhibitor-1 (red) and counterstained with DAPI (blue). The representative images show an overabundance of BI-1 in IPF lung tissue compared to normal. **B)** RNA was extracted from normal (n=7) and IPF (n=7) primary fibroblasts and mRNA expression of BI-1 normalized to 18S was measured via qPCR.

IPF-F are less responsive to ER stress-induced XBP-1 splicing

Since BI-1 is upregulated in IPF and has been shown to be a negative regulator of the IRE1α arm of the UPR, the next objective was to determine if there were any basal differences in IRE1α activity in NHLF and IPF-F. The downstream IRE1α target XBP-1 was used as the readout for IRE1α signaling; activated IRE1α can splice XBP-1, while inactive IRE1α is unable. An accumulation of sXBP-1 in NHLF was observed three hours after administering tunicamycin (Tm). This signal peaked at hour 12 before

diminishing significantly. By hour 24, there was no uXBP-1 remaining in NHLF. On the other hand, no sXBP-1 was observed in IPF-F until 12 hours post-Tm, and the signal that was observed was less intense than the signal displayed by NHLF. The accumulation of sXBP-1 persisted in IPF-F through the 24-hour time point (Figure 8). These differences in XBP-1 splicing indicate that IRE1α signaling activity is diminished in IPF-F compared to NHLF. This reduction in IRE1α signaling in IPF-F could be due to the overabundance of BI-1 observed via IHC and qPCR in Figure 7.

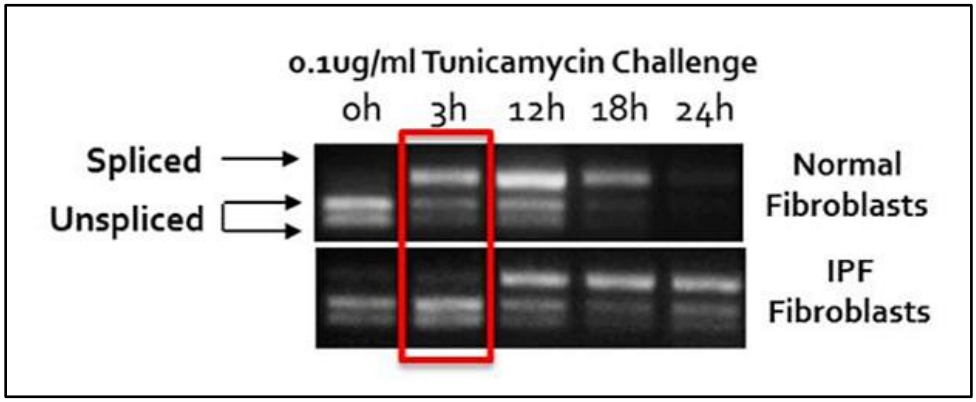

Figure 8: IRE1α splicing activity under in IPF-F and NHLF during ER stress.
RNA was extracted from IPF and normal fibroblasts following a 24-hour 0.1ug/ml tunicamycin challenge. The cDNA of each sample at different time points (0-24 hours) was purified, and PCR was performed using primers that span the spliced region of XBP-1. The unspliced form of XBP-1 contains a *Pst1* restriction enzyme cleave site. The PCR product was digested with *Pst1* for 1 hour at 37°C and resolved on a 1.7% Agarose gel.

Silencing BI-1 promotes the clearance of senescent cells during ER stress conditions

Since we observed an upregulation in BI-1 expression and decreased ability to splice XBP-1 in IPF-F under conditions of ER stress, the next step was to determine the effect of BI-1 knockdown under ER stress. Given the increased expression of BI-1 in senescent cells[28], we hypothesized that ER stress may be a mediator of this effect. Under

basal conditions, 90% of IPF-F show a positive β-gal staining signal. When these cells were dosed with Tm, the percentage of β-gal positive cells decreased to 78%. IPF-F that underwent siRNA transfection targeting BI-1 were 88% positive for β-gal. Under conditions of BI-1 knockdown and Tm challenge, the number of β-gal positive cells dropped to 65% (Figure 9). Since BI-1 silencing caused a 2% reduction in the amount of senescent cells and tunicamycin caused a 12% reduction in the percentage of senescent cells, the 25% decrease seen during the combination of BI-1 silencing and tunicamycin challenge indicates a synergistic relationship between BI-1 knockdown and ER stress This reduction in the percentage of senescent cells when BI-1 was silenced could indicate that BI-1 plays a protective role against ER stress, likely through a reduction in IRE1α signaling, as seen in Figure 8.

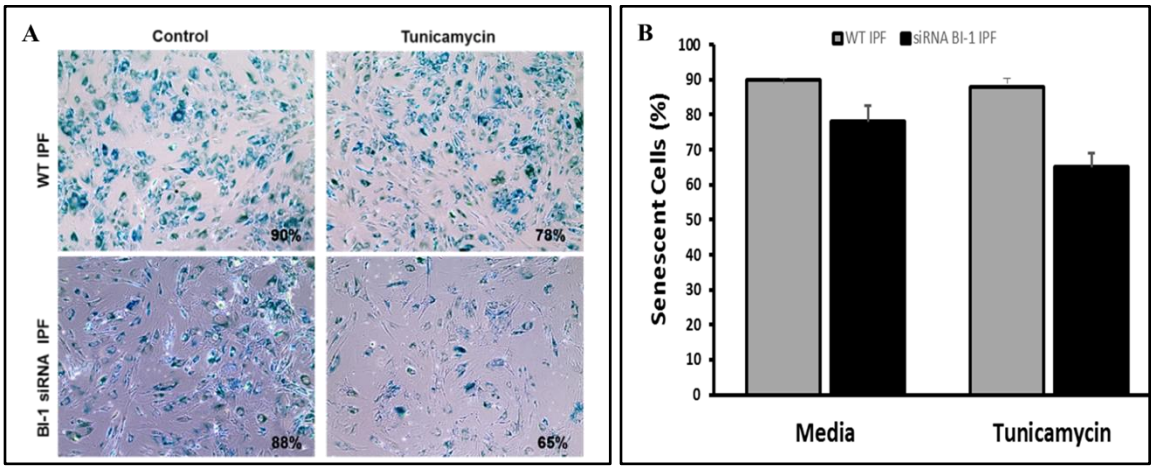

Figure 9: Abundance of senescent cells during ER stress following BI-1 knockdown.
A) Senescent cells (blue-green) were stained for Beta-Gal before and after tunicamycin treatment in unsilenced (WT) and BI-1 knockdown IPF fibroblasts. **B)** Average percentage of senescent cells in 4 representative locations of treatment plates (n=3).

Hypothesis and Aims

Based on these preliminary studies, we hypothesized that the upregulation of BAX Inhibitor-1 (BI-1) in IPF fibroblasts results in decreased activity of IRE1α and BAX, leading to inhibition of ER stress-mediated apoptosis. We planned to test this hypothesis by silencing key UPR proteins BI-1, IRE1α, and BAX, inducing ER stress with tunicamycin, and determining if there were any changes in IRE1α signaling, cell viability, gene expression, or protein expression.

Protocol optimization

0.1 μg/mL tunicamycin induces significant, but not complete cell death

Two concentrations of tunicamycin were tested to determine which would generate significant amounts of stress without decimating cell populations. In the MRC-5 model fibroblast cell line, both the 0.1 μg/mL and 1.0 μg/mL doses resulted in approximately 50% reduction in cell viability. In the A549 cells, the 1.0 μg/mL dose of tunicamycin resulted in 20% reduced cell viability (Figure 10). Given that IPF-F are known to be less sensitive to apoptosis than MRC-5 cells but more sensitive than A549 cells, a dose of 0.1 μg/mL was used for all following experiments requiring the generation of ER stress with tunicamycin.

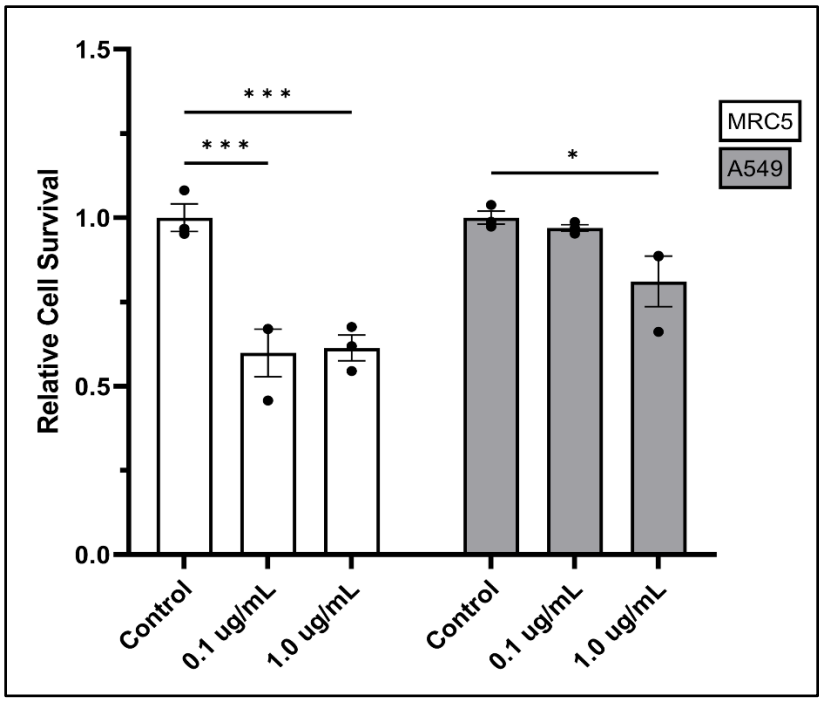

Figure 10: ER stress challenge in MRC-5 and A549 cells.
MRC-5 fibroblasts and A549 alveolar epithelial cells were treated with tunicamycin (0.1 and 1.0 ug/ml) for 24 hours and cell viability was measured using the CCK-8 cell viability kit.

Target protein expression decreased by 20% with 5 μM siRNA

Four concentrations (5, 10, 25, and 50 μM) of IRE1α and BAX siRNA were tested to maximize the silencing effect while minimizing the toxic effects of transfection. The 5 μM transfection showed a 20% decrease in protein expression and increasing the concentration of siRNA from 5 μM to 50 μM did not show a significant difference in the amount of protein silenced. For this reason, all transfections in this study were conducted using a siRNA concentration of 5 μM (Figure 11).

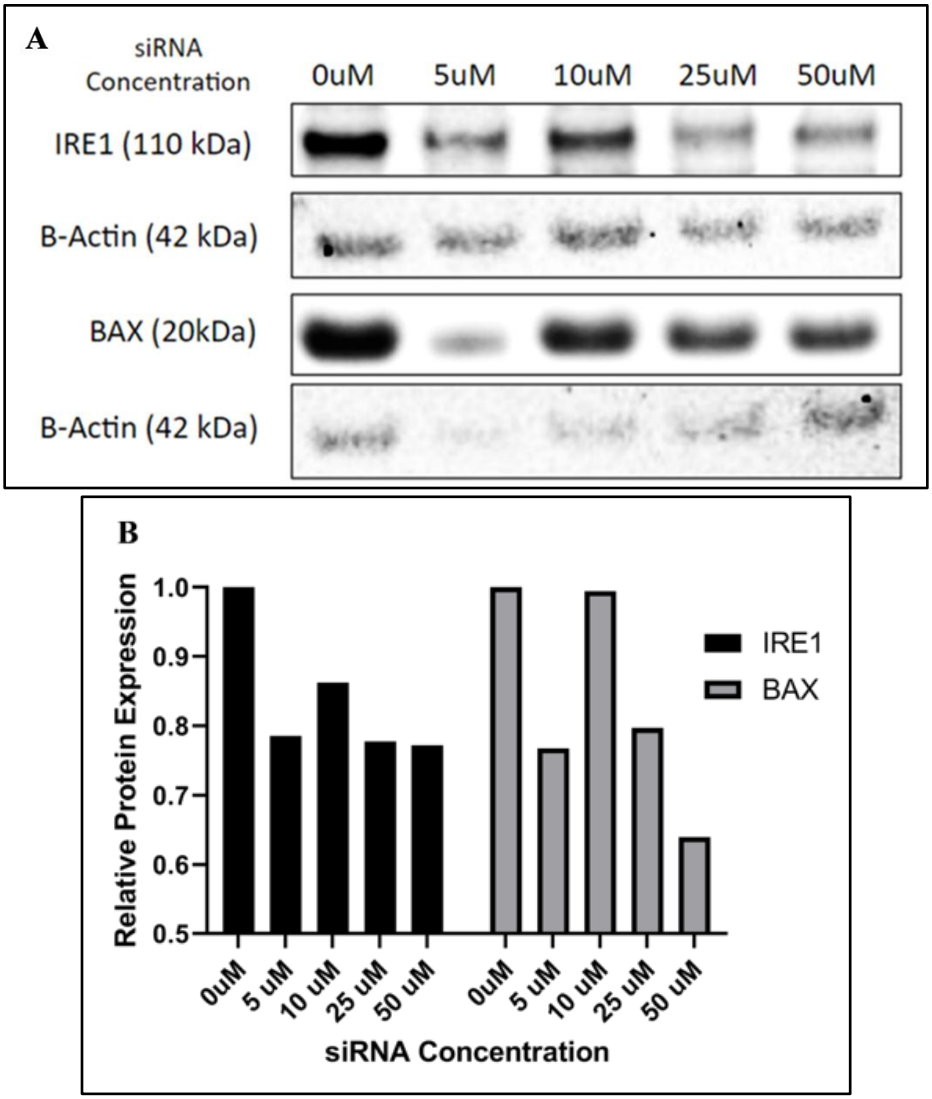

Figure 11: IRE1α and BAX protein expression after siRNA transfection.
IPF fibroblasts were transfected with 4 different concentrations of IRE1α or BAX siRNA (5, 10, 25, and 50 uM) for 24 hours using the Lipofectamine RNAiMax transfection kit. Protein was isolated from each sample and western blotting was performed to measure the expression of IRE1α and BAX, normalized to β-actin expression.

RESULTS

BI-1 silencing promotes splicing of XBP-1 and increased expression of sXBP-1 targets

Given the delay in XBP-1 splicing seen in preliminary studies (Figure 8), we set forth to determine if BI-1 is affecting IRE1α's ability to dimerize and splice XBP-1 by measuring the amount of spliced XBP-1 in fibroblasts after BI-1 knockdown. mRNA isolated from fibroblasts was converted into cDNA and amplified via PCR before being cleaved with the restriction enzyme, *Pst1*. The *Pst1* cleavage site is located within the intron that is removed during IRE1α splicing of XBP-1. Figure 12A depicts the location of the *Pst1* cleavage site relative to the XBP-1 mRNA. The cleavage product was resolved via DNA gel electrophoresis, revealing three bands (Figure 12B). The ratio of sXBP-1 to uXBP-1 was used to determine the percentage of spliced XBP-1. In NHLF treated with BI-1 siRNA, there was an increase in the percentage of sXBP-1 by approximately 5%, while in IPF-F treated with BI-1 siRNA, there was an increase of about 10% (Figure 12C).

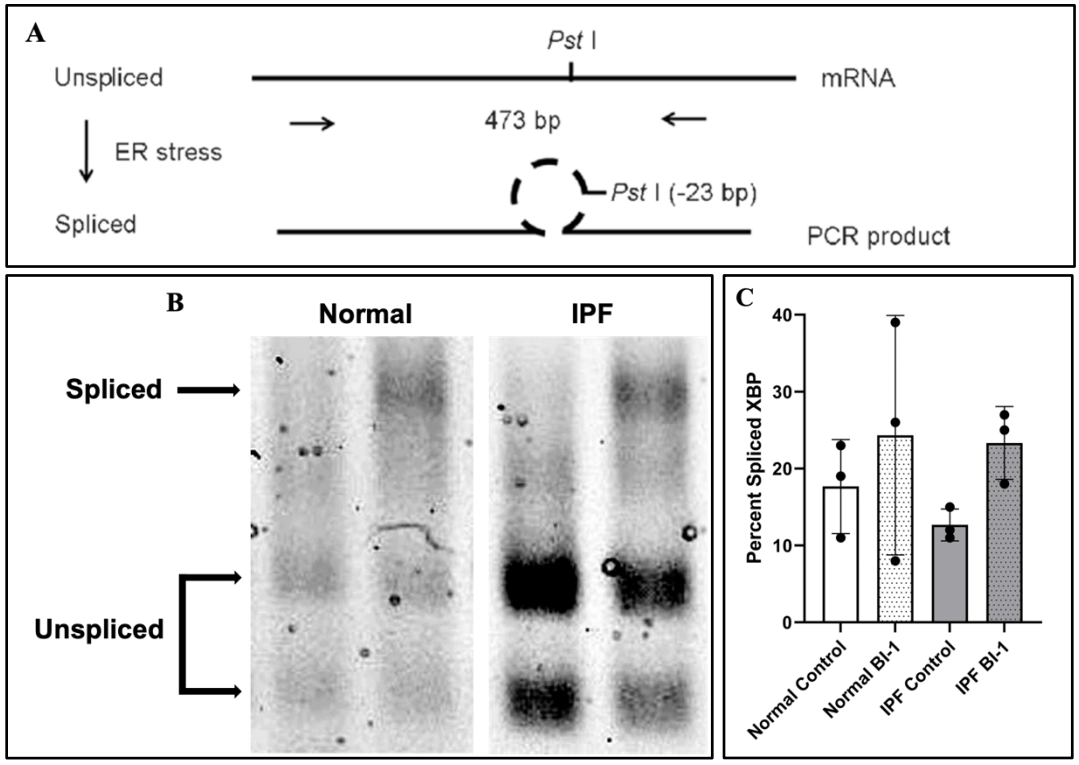

Figure 12: Splicing of XBP1 after BI-1 siRNA transfection.
A) Schematic depicting XBP-1 mRNA splicing detection from Yoo *et al.*, 2017. The unspliced form of XBP-1 contains a *Pst1* cleavage site, while the spliced form does not contain the cleavage site. When digested with *Pst1* and resolved via gel electrophoresis, the spliced form of XBP-1 will appear as a single, large fragment, while the unspliced form will appear as two, small fragments. **B)** Normal and IPF fibroblasts were transfected with BI-1 siRNA for 24 hours using the Lipofectamine RNAiMax transfection kit. RNA was extracted from the cells and cDNA was synthesized and subsequently amplified by PCR. The PCR product was digested with *Pst1* for 1 hour at 37°C and resolved via gel electrophoresis. **C)** The ratio of spliced to unspliced XBP-1 was converted to the percentage of spliced XBP-1 present.

Since the amount of sXBP-1 increased after silencing BI-1, the expression of downstream sXBP-1 target genes was measured via qPCR to functionally confirm the effects of BI-1 silencing. IPF-F and NHLF showed a two-fold increase in the expression of HO1 and a subtle increase in the expression of ERdj4 following BI-1 knockdown, but the expression of SEC61A and ERO1A showed no change (Figure 13). It is important to note that these changes in gene expression were not statistically significant, which could be due to the heterogeneous nature of primary cell culture.

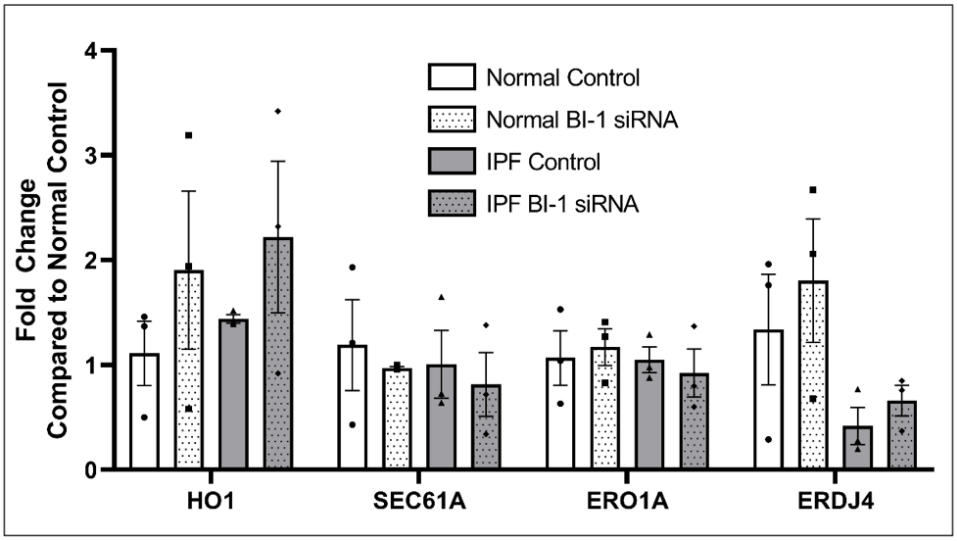

Figure 13: sXBP-1 target gene expression after BI-1 knockdown.
qPCR gene expression analysis of downstream spliced XBP-1 target genes HO1, SEC61A, ERO1A, and ERdj4 in normal and IPF fibroblasts that were transfected with BI-1 siRNA for 24 hours. Expression was normalized to 18S.

siRNA silencing of BAX and IRE1α indicates a differential role for BI-1 in IPF-F and NHLF

BI-1 is also known to inhibit BAX-mediated apoptosis through interactions with pro-survival protein Bcl-2 [25,26,27] (Figure 4), so we also wanted to investigate this mechanism in IPF. To determine the effect that BI-1, IRE1α, and BAX have on fibroblast survival during times of ER stress, IPF-F and NHLF were exposed to tunicamycin for 24 hours after the knockdown of these proteins of interest. The induction of ER stress with tunicamycin resulted in a 20% decrease in cell viability. In IPF-F, the knockdown of BAX resulted in a 50% decrease in cell viability under conditions of ER stress, while the knockdown of BI-1 and IRE1α had no effect (Figure 14A). A different response was observed in NHLF, which showed 25% lower cell viability when BI-1 was silenced and

15% lower cell viability when IRE1α was silenced, but no change when BAX was silenced (Figure 14B)

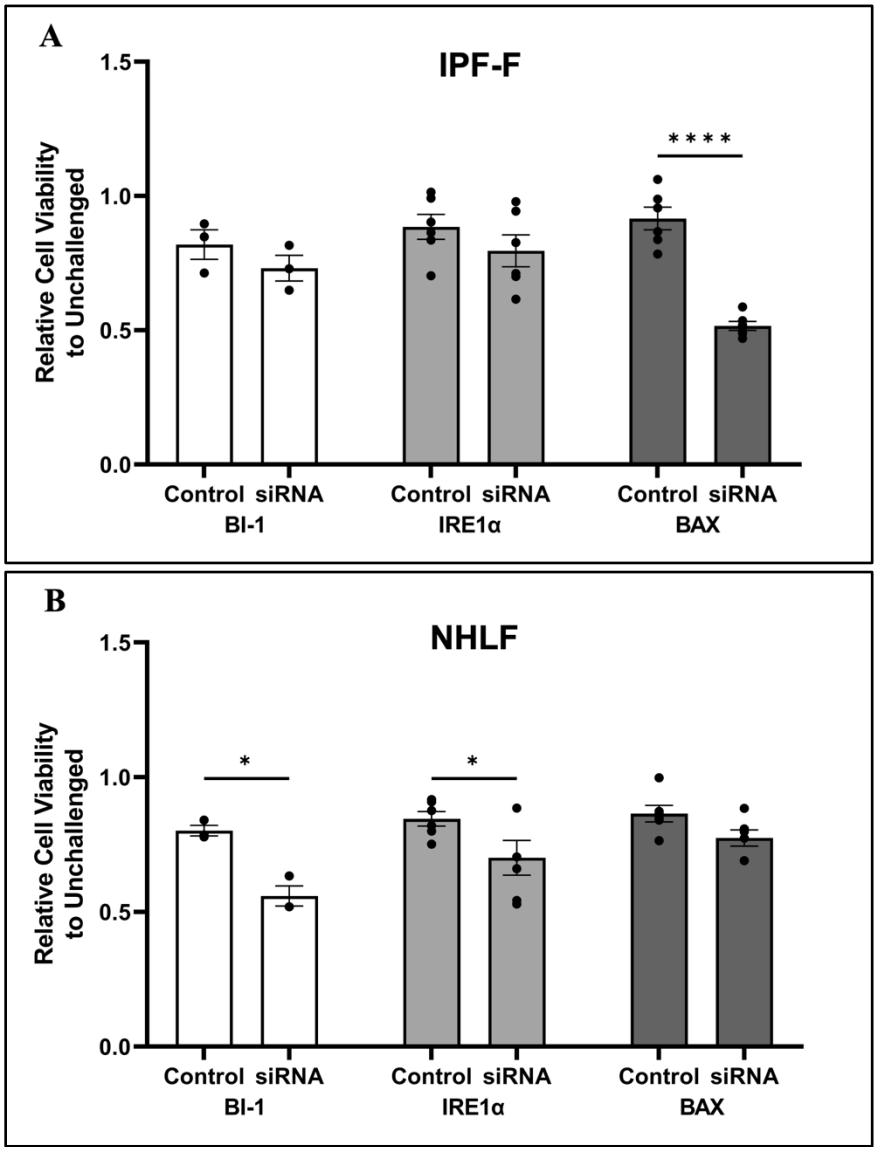

Figure 14: Cell viability of IPF-F and NHLF after transfection and ER stress challenge.
IPF and normal primary fibroblasts were transfected with either BI-1, IRE1α, or BAX siRNA for 24 hours and subsequently challenged with 0.1ug/ml tunicamycin for 24 hours. Relative cell viability compared to unchallenged cells was measured using the CCK-8 cell viability kit.

Tunicamycin induces a strong ER stress response

Given there is a differential response in cell viability to ER stress in IPF-F and NHLF, qPCR was used to determine if there were any changes to UPR target genes HO1, ERO1A, SEC61A, ERdj4, and BiP under conditions of ER stress. Genes involved in protein folding, Erdj4 and BiP, were highly upregulated by 12-16-fold in both IPF-F and NHLF (Figure 15A). sXBP-1 target genes HO1 and ERO1A showed 2.5-fold increased expression, but there was no difference in the expression of SEC61A (Figure 15B). Protein expression analysis of IPF-F and NHLF revealed a similar response with 2-3-fold increases in BiP after tunicamycin dosage, but no change in the amount of CASP3 (Figure 16 A-C).

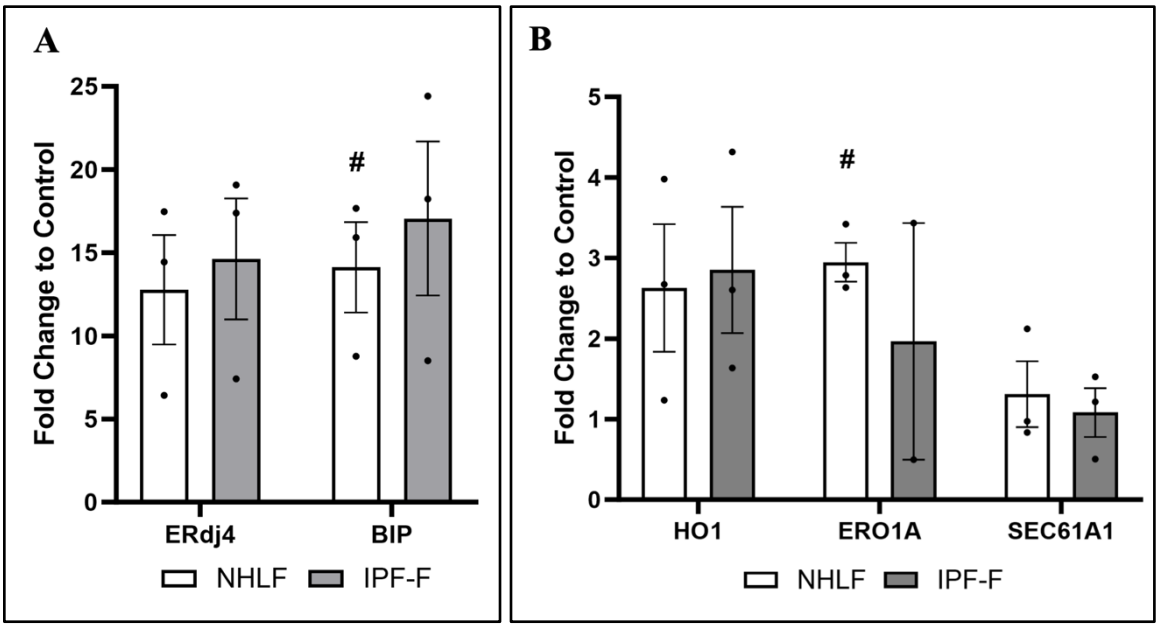

Figure 15: Gene expression of ER stress markers and sXBP-1 targets after ER stress challenge.
IPF and normal fibroblasts were challenged with 0.1ug/ml tunicamycin for 24 hours and RNA was extracted. qPCR was performed to measure the expression of **A)** ER stress markers ERdj4 and BiP; and **B)** sXBP-1 target genes HO1,

ERO1A, and SEC61A. All mRNA expressions are normalized 18S and relative fold change is compared to unchallenged treatment conditions. *# indicates a p-value less than 0.05 compared to unchallenged.*

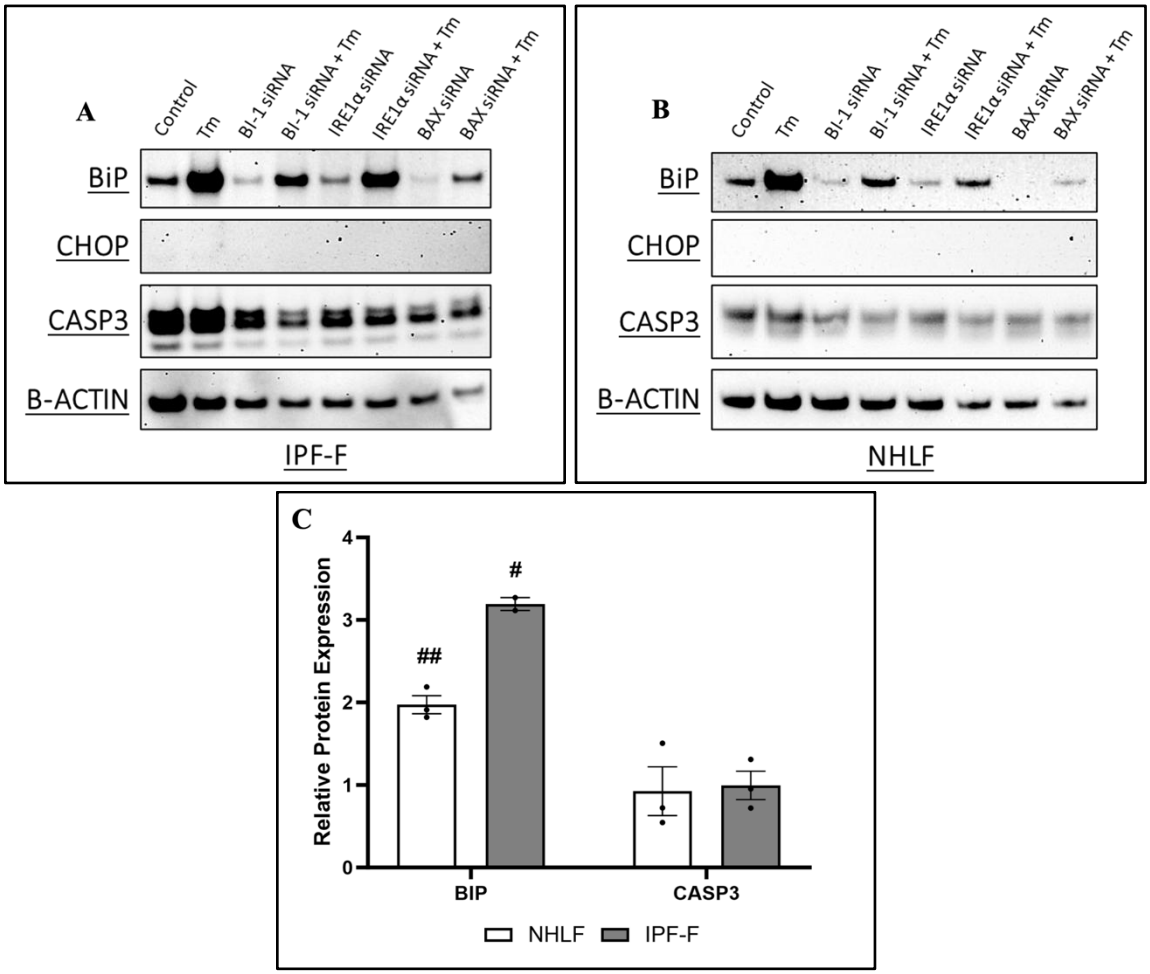

Figure 16: Protein expression of ER stress and apoptosis markers after ER stress challenge.
IPF and normal fibroblasts were challenged with 0.1ug/ml tunicamycin for 24 hours and total protein was isolated. **A)** Western blot analysis was performed to determine the protein expression of ER stress marker BiP, pre-apoptotic signaler CHOP, and apoptotic signaler CASP3/cleaved CASP3, normalized to β-actin. **B)** Relative protein expression was calculated compared to unchallenged cells. CHOP expression was undetected in all cells. *# indicates a p-value less than 0.05 compared to unchallenged cells, and ## indicates a p-value less than 0.01 compared to unchallenged cells.*

Silencing BI-1, IRE1α, and BAX shows differential response in IPF-F and NHLF

Downstream sXBP-1 target gene expression was also measured after siRNA transfection targeting BI-1, IRE1α, and BAX. There were slight increases in the

expression of HO1 and ERdj4 following BAX silencing, but no significant differences between IPF-F and NHLF expression were observed (Figure 17A-B). Protein expression analysis of ER stress-responsive proteins BiP and CASP3 following siRNA transfection targeting BI-1, IRE1α, and BAX showed a differential response in IPF-F and NHLF. BI-1 silenced IPF-F display half the protein expression of BiP compared to unsilenced, while IRE1α silenced IPF-F show a 1.5-fold increase in BiP expression (Figure 18C). NHLF had similar changes in BiP expression when BI-1 was knocked down but had half the BiP expression when IRE1α was silenced as compared to unsilenced (Figure 18D).

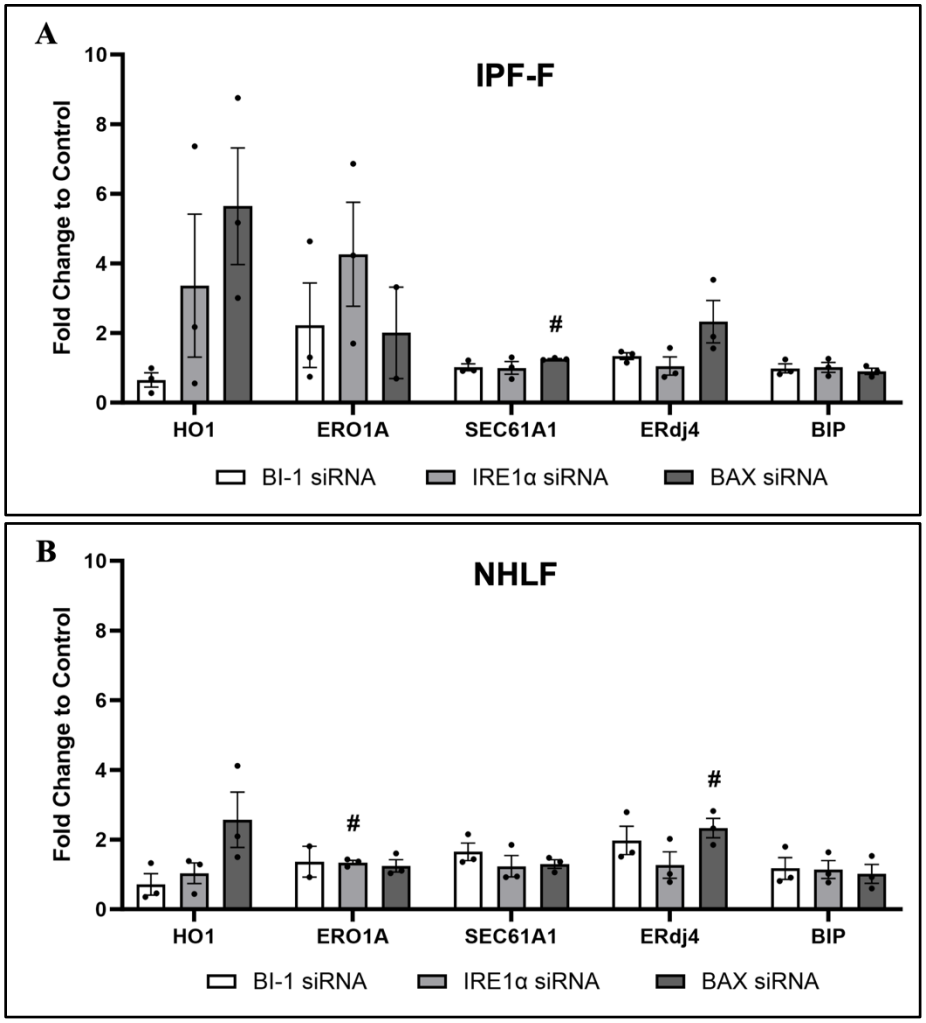

Figure 17: Gene expression of sXBP-1 targets after transfection.
A) IPF and **B)** normal fibroblasts were transfected with BI-1, IRE1α, and BAX siRNA for 24 hours and RNA was extracted. qPCR was performed to measure the gene expression of ER stress markers ERdj4 and BiP, as well as spliced XBP-1 target genes HO1, ERO1A, and SEC61A. All mRNA expressions are normalized 18S and relative fold change is compared to untransfected treatment conditions. *# indicates a p-value less than 0.05 compared to untransfected.*

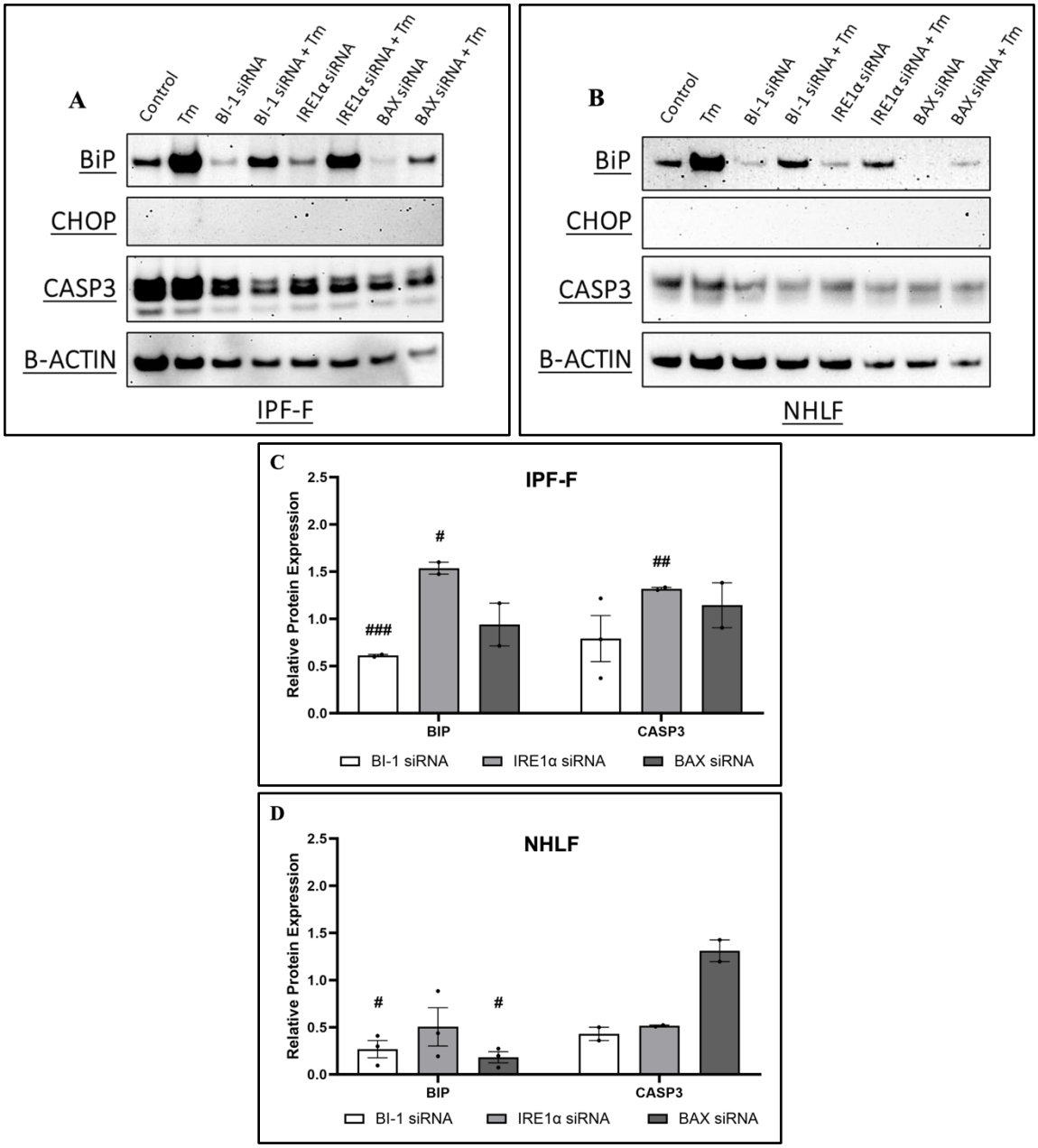

Figure 18: Protein expression of ER stress and apoptosis markers after transfection.
IPF and normal fibroblasts were transfected with BI-1, IRE1α, and BAX siRNA for 24 hours and total protein was isolated. **A)** Western blot analysis was performed to determine the protein expression of ER stress marker BiP, pre-apoptotic signaler CHOP, and apoptotic signaler CASP3/cleaved CASP3, normalized to β-actin. **B)** Relative protein expression was calculated compared to untransfected cells. CHOP expression was undetected in all cells. *### indicates a p-value less than 0.001 compared to untransfected cells*

Silencing BI-1 during ER stress increases gene expression of ER stress markers and downstream sXBP-1 targets

Combining siRNA transfection and tunicamycin-induced ER stress revealed a differential response in downstream sXBP-1 target genes between IPF-F and NHLF. IPF-F showed larger increases in the expression of ER stress markers ERdj4 and BiP (12 and 24-fold, respectively) when BI-1 was silenced, as compared to NHLF. In addition, the expression of HO1 and ERO1A were upregulated 2-fold in IPF-F when BI-1 was silenced but downregulated when IRE1α and BAX were silenced (Figure 19 A-B). In NHLF however, HO1 was 3.5-fold upregulated during BI-1 knockdown but remained unchanged during IRE1α and BAX silencing (Figure 19 C-D).

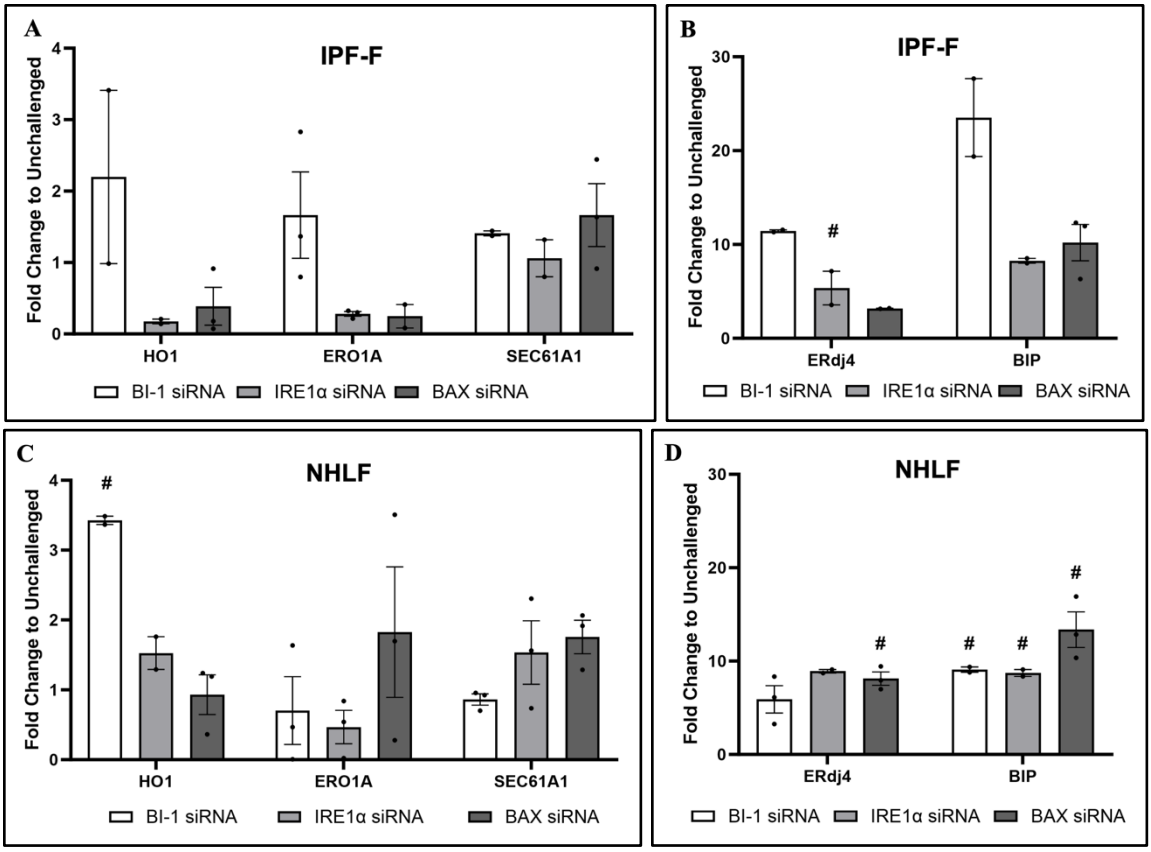

Figure 19: Gene expression of sXBP-1 targets and ER stress markers after transfection and ER stress challenge. A-B) IPF and **C-D)** normal fibroblasts were transfected with BI-1, IRE1α, and BAX siRNA for 24 hours and subsequently challenged with 0.1 ug/ml tunicamycin for 24 hours. RNA was extracted. qPCR was performed to measure the gene expression of ER stress markers ERdj4 and BiP, as well as spliced XBP-1 target genes HO1, ERO1A, and SEC61A. All mRNA expressions are normalized 18S and relative fold change is compared to unchallenged treatment conditions.

Modulating key UPR proteins BI-1, IRE1α, and BAX under conditions of ER stress increases BiP expression, but does not affect CASP3 expression

Lastly, to determine if there were changes in key ER stress and apoptosis pathways that could explain the changes in cell viability, western blot protein expression analysis under conditions of ER stress and siRNA transfection was performed. This revealed a 2-4-fold upregulation of ER stress marker BiP in both IPF-F and NHLF on

average, which was expected. Surprisingly, there was no change in the expression of the proapoptotic marker CASP3 in either group of cells (Figure 20).

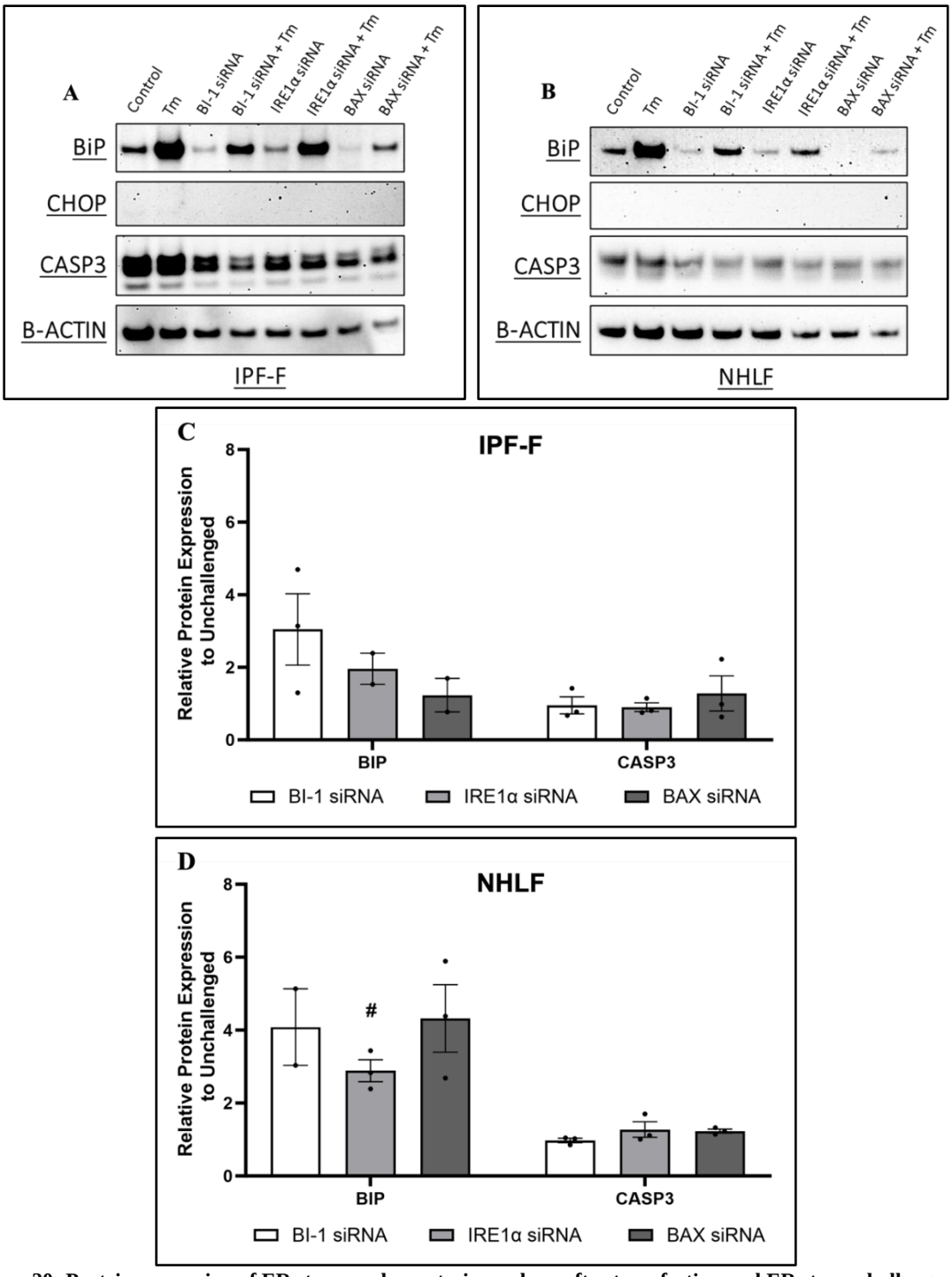

Figure 20: Protein expression of ER stress and apoptosis markers after transfection and ER stress challenge. IPF and normal fibroblasts were transfected with BI-1, IRE1α, and BAX siRNA for 24 hours and total protein was isolated. **A)** Western blot analysis was performed to determine the protein expression of ER stress marker BiP, pre-apoptotic signaler CHOP, and apoptotic signaler CASP3/cleaved CASP3, normalized to β-actin. **B)** Relative protein expression was calculated compared to unchallenged cells. CHOP expression was undetected in all cells.

DISCUSSION

BAX Inhibitor-1 is a six-transmembrane domain-containing protein that has been shown to negatively regulate the important ER stress sensor IRE1α and the key proapoptotic protein BAX [25,26]. BI-1 is thought to work through direct interaction with IRE1α, which would prevent the proper dimerization required for IRE1α activation, autophosphorylation, proper splicing of XBP-1, and downstream IRE1α signaling[25,26,27]. A mechanism of this type would theoretically provide cells that overexpress BI-1 with increased resistance to ER stress by inhibiting one of the three pathways that activate the unfolded protein response (Figure 4).

We first set forth to characterize the expression of BI-1 in the IPF lung. It was seen that BI-1 is expressed at higher levels in lung tissue sections and fibroblasts isolated from IPF patients, as compared to normal lungs (Figure 7). IRE1α activity during ER stress was also shown to be delayed in IPF-F, as it took longer to begin splicing XBP-1 in IPF-F than in NHLF (Figure 8). We believe this could be due to the increased expression of BI-1 within the IPF lung. When BI-1 was silenced under conditions of ER stress, there was a smaller percentage of senescent cells, indicating that BI-1 could serve a protective role against ER stress in these senescent cells (Figure 9).

To further demonstrate that BI-1 negatively regulates IRE1α, the ability of IRE1α to splice XBP-1 was examined following BI-1 knockdown. In both IPF-F and NHLF, sXBP-1 was more abundant when BI-1 was silenced (Figure 12). Furthermore, downstream gene targets of sXBP-1 were altered following BI-1 knockdown (Figure 13).

Taken together, these data suggest that high expression levels of BI-1 prevent IRE1α from functioning properly.

To further characterize the potential protective mechanisms of BI-1 in IPF-F, we silenced BI-1, IRE1α, and BAX under conditions of ER stress. Interestingly, silencing BI-1 and IRE1α in IPF-F had no significant effect on cell viability, but BAX knockdown resulted in a nearly 50% decrease in cell viability. The opposite trend was observed in NHLF; BAX knockdown had no significant effect on cell viability, while BI-1 and IRE1α silencing reduced cell viability by 50% and 40%, respectively (Figure 14).

The reason for this differential response needed to be elucidated, so we measured the expression changes of UPR target genes HO1, ERO1A, SEC61A, ERdj4, and BiP. These genes are direct targets of the activated transcription factor sXBP-1, so their expression would provide valuable information about UPR activity. In addition, the expression of the chaperone protein BiP was used as a marker for ER stress, the expression of CHOP was used as a marker for pre-apoptotic signaling, and the expression of CASP3 was used as a marker for apoptotic signaling.

The first step was to determine how the cells respond to an ER stress challenge. As expected, there was a strong increase in the gene expression of chaperone proteins ERdj4 and BiP. This was confirmed by protein expression analysis, which showed an increase in BiP, but CASP3 expression remained unchanged. There was no CHOP expression observed under any treatment combinations. This indicates that the low-dosage tunicamycin used induced significant amounts of ER stress but did not initiate a pro-apoptotic cascade (Figure 15).

Investigating the effect of BI-1, IRE1α, and BAX siRNA transfection on IPF-F and NHLF gene expression did not reveal any significant differences. However, the protein expression of BiP displayed a differential response. IPF-F had decreased expression of BiP when BI-1 was silenced, but when IRE1α was silenced, there was an increase in BiP expression. NHLF showed lower BiP with all silencing conditions (Figure 16).

When the combination of siRNA transfection and tunicamycin challenge was performed, a robust ER stress response was observed. The expression of sXBP-1 target genes was more upregulated in IPF-F that had BI-1 silenced. Chaperone protein gene expression of ERdj4 and BiP was upregulated in both IPF-F and NHLF, as expected under conditions of ER stress. This upregulation was exaggerated in IPF-F which had BI-1 silenced. These data taken together point to BI-1 attenuating ER stress responses in IPF-F; when BI-1 was silenced, IPF-F were more responsive (Figure 17). Protein expression of BiP under the same conditions was also upregulated in both IPF-F and NHLF. Interestingly, there was no change in CASP3 expression (Figure 18). The lack of cleaved CASP3 protein expression points to the changes in cell viability being due to a CASP3-independent mechanism.

CONCLUSION

BAX Inhibitor-1's role in the regulation of the unfolded protein response is still in need of further characterization, but this study confirms that BI-1 is a negative regulator of ER stress-induced apoptosis. Specifically, BI-1 seems to attenuate the propagation of ER stress signaling through the IRE1α arm of the UPR. IPF fibroblasts express BI-1 at much higher levels than their normal counterparts, which could point to the small changes in cell viability that were observed when BI-1 was silenced. Since there was only about a 20-25% reduction in protein expression with siRNA transfection, the remaining amount of BI-1 in IPF-F was likely enough to still protect against ER stress.

There are a couple of areas where this study is limited. First, the siRNA transfections yielded relatively low silencing efficiency – only about 20-25% knockdown. Any functional data that was collected, like cell viability or changes in gene expression, are highly dependent on the amount of remaining protein following transfection. The results presented in this study could likely be more exaggerated with a more efficient silencing method. Secondly, the unfolded protein response is an incredibly complex pathway with many different signal pathways that intersect. This study only selected a small portion of these signaling molecules as gene expression and protein expression readouts.

A key question that has yet to be answered is whether BI-1 and IRE1α can make direct protein-protein interactions, as is hypothesized. Answering this question using co-immunoprecipitation would greatly benefit the field. In addition, using an alternate

silencing method, like CRISPR or small molecule inhibitors, could provide more robust silencing efficiency. Lastly, it seems necessary to increase the amount of UPR readouts to provide a clearer picture of BI-1's role in IPF. Choosing other downstream XBP-1 target genes and additional apoptotic signaling mechanisms would be most beneficial. Investigating signaling molecules at key UPR pathway intersections would also provide information about potential compensatory signaling from the other UPR pathways.

REFERENCES

1. Martinez FJ, Collard HR, Pardo A, et al. Idiopathic pulmonary fibrosis. *Nat Rev Dis Primers*. 2017;3(1):17074. doi:10.1038/nrdp.2017.74

2. Idiopathic Pulmonary Fibrosis | NHLBI, NIH. Accessed November 27, 2021. https://www.nhlbi.nih.gov/health-topics/idiopathic-pulmonary-fibrosis

3. Hinz B, Lagares D. Evasion of apoptosis by myofibroblasts: a hallmark of fibrotic diseases. *Nat Rev Rheumatol*. 2020;16(1):11-31. doi:10.1038/s41584-019-0324-5

4. Wolters PJ, Collard HR, Jones KD. Pathogenesis of Idiopathic Pulmonary Fibrosis. *Annu Rev Pathol*. 2014;9:157-179. doi:10.1146/annurev-pathol-012513-104706

5. Raghu G, Weycker D, Edelsberg J, Bradford WZ, Oster G. Incidence and Prevalence of Idiopathic Pulmonary Fibrosis. *Am J Respir Crit Care Med*. 2006;174(7):810-816. doi:10.1164/rccm.200602-163OC

6. Spagnolo P, Kropski JA, Jones MG, et al. Idiopathic pulmonary fibrosis: disease mechanisms and drug development. *Pharmacol Ther*. 2021;222:107798. doi:10.1016/j.pharmthera.2020.107798

7. Fell CD, Martinez FJ, Liu LX, et al. Clinical Predictors of a Diagnosis of Idiopathic Pulmonary Fibrosis. *Am J Respir Crit Care Med*. 2010;181(8):832-837. doi:10.1164/rccm.200906-0959OC

8. Seibold MA, Wise AL, Speer MC, et al. A Common MUC5B Promoter Polymorphism and Pulmonary Fibrosis. *N Engl J Med*. 2011;364(16):1503-1512. doi:10.1056/NEJMoa1013660

9. López-Otín C, Blasco MA, Partridge L, Serrano M, Kroemer G. The Hallmarks of Aging. *Cell*. 2013;153(6):1194-1217. doi:10.1016/j.cell.2013.05.039

10. Angelidis I, Simon LM, Fernandez IE, et al. An atlas of the aging lung mapped by single cell transcriptomics and deep tissue proteomics. *Nat Commun*. 2019;10(1):963. doi:10.1038/s41467-019-08831-9

11. Schneider JL, Rowe JH, Garcia-de-Alba C, Kim CF, Sharpe AH, Haigis MC. The aging lung: Physiology, disease, and immunity. *Cell*. 2021;184(8):1990-2019. doi:10.1016/j.cell.2021.03.005

12. Dzau VJ, Finkelman EM, Balatbat CA, Verdin EM, Pettigrew RI. Achieving healthy human longevity: A global grand challenge. *Science Translational Medicine*. 2020;12(566):eabd3816. doi:10.1126/scitranslmed.abd3816

13. Álvarez D, Cárdenes N, Sellarés J, et al. IPF lung fibroblasts have a senescent phenotype. *Am J Physiol Lung Cell Mol Physiol*. 2017;313(6):L1164-L1173. doi:10.1152/ajplung.00220.2017

14. Habiel D, Hohmann MSN, Espindola M, et al. DNA-PKcs modulates progenitor cell proliferation and fibroblast senescence in idiopathic pulmonary fibrosis. *BMC Pulmonary Medicine*. 2019;19. doi:10.1186/s12890-019-0922-7

15. Rhinn M, Ritschka B, Keyes WM. Cellular senescence in development, regeneration and disease. *Development*. 2019;146(20):dev151837. doi:10.1242/dev.151837

16. Roger L, Tomas F, Gire V. Mechanisms and Regulation of Cellular Senescence. *Int J Mol Sci*. 2021;22(23):13173. doi:10.3390/ijms222313173

17. Di Micco R, Krizhanovsky V, Baker D, d'Adda di Fagagna F. Cellular senescence in ageing: from mechanisms to therapeutic opportunities. *Nat Rev Mol Cell Biol*. 2021;22(2):75-95. doi:10.1038/s41580-020-00314-w

18. Pluquet O, Pourtier A, Abbadie C. The unfolded protein response and cellular senescence. A review in the theme: cellular mechanisms of endoplasmic reticulum stress signaling in health and disease. *Am J Physiol Cell Physiol*. 2015;308(6):C415-425. doi:10.1152/ajpcell.00334.2014

19. Szegezdi E, Logue SE, Gorman AM, Samali A. Mediators of endoplasmic reticulum stress-induced apoptosis. *EMBO Rep*. 2006;7(9):880-885. doi:10.1038/sj.embor.7400779

20. Gorman AM, Healy SJM, Jäger R, Samali A. Stress management at the ER: Regulators of ER stress-induced apoptosis. *Pharmacology & Therapeutics*. 2012;134(3):306-316. doi:10.1016/j.pharmthera.2012.02.003

21. Tanjore H, Blackwell TS, Lawson WE. Emerging evidence for endoplasmic reticulum stress in the pathogenesis of idiopathic pulmonary fibrosis. *Am J Physiol Lung Cell Mol Physiol*. 2012;302(8):L721-729. doi:10.1152/ajplung.00410.2011

22. Hetz C. The unfolded protein response: controlling cell fate decisions under ER stress and beyond. *Nature Reviews Molecular Cell Biology*. 2012;13(2):89-102. doi:10.1038/nrm3270

23. Yoshida H, Uemura A, Mori K. pXBP1(U), a negative regulator of the unfolded protein response activator pXBP1(S), targets ATF6 but not ATF4 in proteasome-mediated degradation. *Cell Struct Funct*. 2009;34(1):1-10. doi:10.1247/csf.06028

24. Kimata Y, Oikawa D, Shimizu Y, Ishiwata-Kimata Y, Kohno K. A role for BiP as an adjustor for the endoplasmic reticulum stress-sensing protein Ire1. *J Cell Biol*. 2004;167(3):445-456. doi:10.1083/jcb.200405153

25. Lisbona F, Rojas-Rivera D, Thielen P, et al. BAX Inhibitor-1 Is a Negative Regulator of the ER Stress Sensor IRE1α. *Molecular Cell*. 2009;33(6):679-691. doi:10.1016/j.molcel.2009.02.017

26. Robinson KS, Clements A, Williams AC, Berger CN, Frankel G. Bax Inhibitor 1 in apoptosis and disease. *Oncogene*. 2011;30(21):2391-2400. doi:10.1038/onc.2010.636

27. Xu Q, Reed JC. Bax Inhibitor-1, a Mammalian Apoptosis Suppressor Identified by Functional Screening in Yeast. *Molecular Cell*. 1998;1(3):337-346. doi:10.1016/S1097-2765(00)80034-9

28. Ishikawa T, Watanabe N, Nagano M, Kawai-Yamada M, Lam E. Bax inhibitor-1: a highly conserved endoplasmic reticulum-resident cell death suppressor. *Cell Death Differ*. 2011;18(8):1271-1278. doi:10.1038/cdd.2011.59

BIOGRAPHY

Durwood Moore graduated from Arcadia High School, Oak Hall, Virginia, in 2016. He graduated cum laude with his Bachelor of Science degree in Biology from George Mason University, Fairfax, Virginia, in 2019.